International Journal of Pharmaceutics 648 (2023) 123566

Contents lists available at ScienceDirect

International Journal of Pharmaceutics

journal homepage: www.elsevier.com/locate/ijpharm

A Nanoemulgel for Nose-to-Brain delivery of Quetiapine – QbD-Enabled formulation development & *in-vitro* characterization

Dnyandev Gadhave, Mural Quadros, Akanksha R. Ugale, Mimansa Goyal, Vivek Gupta *

Department of Pharmaceutical Sciences, College of Pharmacy and Health Sciences, St. John's University, 8000 Utopia Parkway, Queens, NY 11439, USA

ARTICLE INFO

Keywords:
Chitosan Nanoemulgel
Quetiapine
Mental disorders
Nose-to-brain delivery
RPMI-2650 cells
Cellular permeation
Transepithelial electrical resistance

ABSTRACT

Second-generation antipsychotics, quetiapine hemifumarate (QF), exhibited highly active against negative and positive signs of psychosis. However, contemporary reports have shown that long-term therapy with QF causes lethal thrombocytopenia and leukopenia. Hence, to circumvent the drawbacks of available therapies, the current work aimed to design a QF-loaded biodegradable nanoemulsion (QF-NE) with suitable surface charge modification by poloxamer-chitosan and evaluate its targeting efficiency against RPMI-2650 cell lines. QF-loaded poloxamer-chitosan in-situ gel (QF-Nanoemulgel) was formulated through the O/W emulsification aqueous titration technique and optimized using the QbD approach. Optimized QF-Nanoemulgel subjected to evaluate for globule size, PDI, zeta potential, %T, viscosity, %EE, and ex-vivo mucoadhesive strength were found to be 15.0 ± 0.3 nm, 0.05 ± 0.001, −18.3 ± 0.2 mV, 99.8 ± 0.8 %, 13.5 ± 2.1 cP, 69.0 ± 1.5 %, and 43.7 ± 1.5 g, respectively. QF-Nanoemulgel revealed sustained release and obeyed zero-order kinetics compared to QF-NE and QF-suspension. Additionally, nanoformulations treated blood samples did not cause hemolytic activity compared to drug and negative control after 10 h treatment. Further, in-vitro cytotoxicity, cellular uptake, and permeation of 12.5 and 25 μM QF-Nanoemulgel were assessed on RPMI-2650 cells and discovered nontoxic with 0.55 ± 0.02 μg and 1.1 ± 0.04 μg cellular permeation, respectively, which ensured the safety and potency of QF-Nanogel. Current research revealed the successful development of intranasal QF-Nanoemulgel as a novel dosage form for the safe and effective delivery of QF in schizophrenia patients.

1. Introduction

Schizophrenia is a debilitating mental condition that adversely influences the patient's perceptions, feelings, manners, and cognitive abilities, frequently resulting in suicidal tendencies due to significant mood swings (Gadhave et al., 2021b; Seju et al., 2011). Therapy of schizophrenia is focused on symptomatic management, and is a challenging task for formulation scientists due to hurdles associated with penetration across the blood–brain barrier (BBB) (Fornaguera et al., 2015; Qu et al., 2021). Therefore, current treatment and delivery strategies for mental conditions such as schizophrenia appear to have failed in this prospect.

The second-generation atypical antipsychotic quetiapine hemifumarate (QF), is a FDA-approved medication for mental illnesses such as schizophrenia (Shah et al., 2016; Zhou et al., 2020). QF is highly potent against positive and negative symptoms of schizophrenia. However, previously published reports suggest incidences of fatal leukopenia and thrombocytopenia following chronic treatment of schizophrenic patients with QF (Arslan et al., 2016; Crépeau-Gendron and L'Heureux, 2015; Fan et al., 2015; Ravi Shankar, 2007). QF interacts with an enzyme, cytochrome P450 2D6; and is catalyzed in 7-hydroxyquetiapine, which is further oxidized by human myeloperoxidase/H_2O_2 to produce reactive radicals and a reactive quinone-imine (Li and Cameron, 2012). These radicals unwantedly reduce the white blood cell count and result in leukopenia and thrombocytopenia.

Current oral tablet formulations of QF exhibit very limited bioavailability of approximately 9 % (Zhou et al., 2020). Hence, excessive doses and frequent administrations of QF are needed to maintain the drug concentration within the therapeutic window. In contrast, oral QF is absorbed directly into the blood from the GI epithelium, which may result in unintended hematological toxicities (Shah et al., 2016). QF delivery with existing formulations is very difficult due to the dense network of endothelial cells i.e., the blood–brain barrier (BBB) in the central nervous system (CNS), which acts as a biological barrier and limits the administration of therapies to the brain (Gadhave et al., 2022; Li and Cameron, 2012). Alternatively,

* Corresponding author at: College of Pharmacy and Health Sciences, St. John's University, 8000 Utopia Parkway, Queens, NY 11439, USA.
E-mail address: guptav@stjohns.edu (V. Gupta).

https://doi.org/10.1016/j.ijpharm.2023.123566
Received 6 September 2023; Received in revised form 26 October 2023; Accepted 29 October 2023
Available online 2 November 2023

intravenous formulations help to overcome the bioavailability concerns by circumventing extensive first-pass elimination. However, parenteral delivery appears to fail in amplifying adequate QF concentrations in the brain because of the tight junctions of BBB (Pathak et al., 2014). Therefore, it is imperative to improve and advance drug delivery approaches, ensuring the site-specific, safe, and efficient transport of QF to targeted sites by a non-invasive route of administration.

Nowadays, nose-to-brain administration strategies have enticed substantial attention among researchers regarding CNS therapies, owing to their potential to promote direct therapeutic delivery from the nostril to the brain, circumventing the formidable BBB (Bruinsmann et al., 2022; Cunha et al., 2022; Gadhave et al., 2023). In this context, numerous pathways facilitate drug delivery from the nose to CNS such as the olfactory, lymphatic, and trigeminal nerve pathways (Gadhave et al., 2022). Intranasal (IN) route has proven to be a potential asset for transporting antipsychotics effectively to the brain through exposed nerve endings (Gadhave et al., 2019b). Furthermore, this approach facilitates non-invasive administration and direct CNS distribution through bypassing first-pass elimination and enzymatic degradation (Banks, 2012). Additionally, it provides some advantages like reduction of dosage and dosing intensity which increase patient comfort and compliance. However, IN administration encounters certain limitations including mucociliary clearance, a protective mechanism that expedites the rapid elimination of applied delivery systems from the nasal cavity (Bhavna et al., 2014). These nasal defensive mechanisms shorten the nasal residence time for applied formulations, thus impeding drug permeation through intranasal route (Yu et al., 2018). To circumvent this issue, incorporation of mucoadhesive and gel-forming polymers such as chitosan and poloxamer into IN formulations has shown the potential to prolong drug localization at the application site and thereby enhance brain penetration (Qu et al., 2021).

According to previously published studies, lipid-based nanoformulations have demonstrated their superior potency in delivering therapeutics to the CNS compared to conventional formulations (Fornaguera et al., 2015; Raman et al., 2022). Several formulation experts have emphasized the suitability of lipid-based nanoparticles i.e., nanoemulsion (NE) for drug delivery in neurological disorders due to their advantageous features including nanometric size (10–100 nm), adequate biodegradability, superior biocompatibility, controlled release capacity, and efficient drug entrapment and loading capabilities (Ahmad, 2017; Raman et al., 2022). Further, NE serves as a prominent carrier/vector for mRNA, proteins, DNA, therapeutic agents, and vitamins. Chitosan is a natural polysaccharide widely utilized in biomedical applications due to its adequate biocompatibility, notable safety, substantial biological activity, and minimal immunogenicity (Ahmad, 2017; Bruinsmann et al., 2022; Tong et al., 2017). Notably, Chitosan, a natural gelling agent, has a remarkable quality of forming a gel in the presence of mucin, primarily obtained in nasal secretions, and to interact electrostatically with physiological fluid at pH 2.5 and 6.4, resulting in mucoadhesion (Ahmad et al., 2022). Simultaneously, poloxamer 407 has been incorporated to design thermoresponsive in-situ gels, facilitating the consistency and cohesiveness of the formulation (Gadhave et al., 2023; Yu et al., 2018). Many researchers have frequently used a combination of ionic and thermo-responsive gelling systems for nose-to-brain delivery, where the formulation exists as a liquid at room temperature and transition into a gel at physiological temperature (34 °C) (Gadhave et al., 2021b; Yu et al., 2018).

The current work endeavors to design a QF-loaded biodegradable nanoemulsion (QF-NE) formulation subjected to appropriate surface charge modification with poloxamer-chitosan conjugation and examine its brain-targeting potential, to surmount the limitations of conventional QF therapies. Current work explored to develop QF-nanoemulsion-loaded chitosan-poloxamer 407 in-situ gel (QF-Nanoemulgel) by emulsification and water titration method. A QbD approach was utilized to develop QF-NE formulation, which facilitates highly precise formulation while reducing development costs and time. Moreover, the QF-NE and QF-Nanoemulgel were then meticulously characterized for globule size, ex-vivo mucoadhesion, rheological behaviors, surface charge, hematological toxicities, surface morphology, accelerated stability, in-vitro release, in-vitro cytotoxicity, in-vitro cellular uptake, and permeation studies in nasal epithelial cell lines to demonstrate the safety and targeting potential of the developed lipid-based nanoformulations.

2. Materials and methods

2.1. Materials

Quetiapine hemifumarate (QF) was purchased from Cayman Chemical Company (Ann Arbor, MI, USA). Labrafil M 1944 CS, Maisine 35–1, Peceol, Labrasol, and Transcutol HP were received as gift samples from Gattefosse (Paramus, NJ, USA), Capmul MCM was received as a gift sample from ABITEC Corporation (Columbus, OH, USA). Coumarin-6, HPLC grade acetonitrile (ACN), 3-(4,5-dimethylthiazol-2-yl)-2,5-diphenyltetrazolium bromide (MTT), dimethyl sulfoxide (DMSO), and UPLC water were procured from Fisher Scientific (Hampton, NH, USA). Kolliphor® 407 was received as a gift sample from BASF Corporation (Tarrytown, NY, USA). Glycol chitosan and Tween 20 were purchased from MedChem Express (Monmouth Junction, NJ, USA). The nasal epithelial cell line (RPMI-2650) was purchased from ATCC (Manassas, VA, USA) and cultured in an EMEM medium augmented with 1 % antibiotics (penicillin–streptomycin) and 10 % FBS (Atlanta Biologicals). Further, cell lines were incubated at 90–100 % relative humidity and 37 °C/5% CO_2. Rat nasal mucosa was isolated from euthanized rats at St. John's University Animal Care Center for mucoadhesive strength study.

2.2. UPLC analytical method development for QF

A reverse-phase liquid chromatography technique was developed for quantifying QF using UPLC (Waters, Milford, MA, USA). The column used was XBridge® BEH Shield RP18 2.5 μm (3.0 × 100 mm). The mobile phase combined an organic phase of ACN and an aqueous phase of 0.1 % orthophosphoric acid (OPA) in a ratio of 75:25 with a flow rate of 0.3 mL/min. The wavelength used for detection was 294 nm. The data was processed using Empower 3.0 software (Waters, MA, USA).

2.3. Screening of Oils, Surfactants, and co-surfactant for QF-NE formulation

The solubility of QF was estimated in various oils (Capmul MCM, Oleic acid, Peceol, Labrafil M 1944 CS, Maisine CC, Leuroglycol 90, Caproyl 90, and Labrafac PG, etc.), surfactants (Tween 80, Span 80, Cremophor RH 40, Tween 20, and Labrasol, etc.), and co-surfactants (Polyethylene glycol 400, Ethanol, Transcutol HP, and Propylene glycol, etc.) using a saturation solubility approach. 10 mg of QF was added in 10 mL of each vehicle at every time in a centrifuge tube to attain an equilibrium and was shaken at room temperature at 250 rpm for 72 h using an orbital shaker, after which the mixture was centrifuged at 10,000 × g for 30 min at 4 °C. The supernatant was isolated and filtered through a 0.45 μm membrane filter and diluted with acetonitrile. Solubilized QF amount was quantified using the UPLC method described earlier.

2.4. Construction of Pseudo-Ternary phase diagrams

Pseudo-ternary phase diagrams were designed to demonstrate the appropriate NE region through an emulsification aqueous titration approach. Briefly, co-surfactants and surfactants were combined according to a predetermined weight composition (1:1, 2:1, and 1:2). The selected oil was incorporated into predefined S_{mix} ratios (9:1, 8:2, 7:3, 6:4, 5:5, 4:6, 3:7, 2:8, and 1:9 w/w) for the phase diagram design. Further, each (oil-S_{mix}) combination was titrated with an appropriate amount of water while continuously stirring. After equilibrium, test

Table 1
The experimental design layout created for 17 batches of QF-NE by Box-Behnken statistical design.

Sr. No.	Formulation factors			Responses		
	Oil (mL)	S_{mix} (mL)	Water (mL)	Globule size (nm)	PDI	Zeta potential (mV)
F1	1	1	0	54.7 ± 1.2	0.09 ± 0.003	−5.3 ± 0.2
F2	0	0	0	22.1 ± 0.4	0.06 ± 0.002	−5.5 ± 0.1
F3	0	0	0	21.9 ± 0.8	0.05 ± 0.004	−5.6 ± 0.3
F4	0	0	0	23.8 ± 0.3	0.06 ± 0.003	−4.8 ± 0.1
F5	0	1	1	16.3 ± 0.2	0.05 ± 0.001	−7.2 ± 0.4
F6	0	0	0	21.9 ± 0.6	0.06 ± 0.003	−5.3 ± 0.2
F7	0	1	−1	22.3 ± 0.5	0.05 ± 0.002	−5.1 ± 0.2
F8	1	0	−1	89.0 ± 1.9	0.30 ± 0.02	−3.4 ± 0.4
F9	−1	0	1	12.3 ± 0.4	0.04 ± 0.002	−10.4 ± 0.4
F10	0	−1	1	25.8 ± 0.7	0.06 ± 0.003	−4.1 ± 0.3
F11	1	−1	0	96.3 ± 2.1	0.51 ± 0.04	−3.1 ± 0.1
F12	0	0	0	24.1 ± 0.3	0.04 ± 0.001	−5.8 ± 0.2
F13	−1	0	−1	14.0 ± 0.2	0.04 ± 0.003	−15.3 ± 0.3
F14	1	0	1	70.3 ± 1.4	0.28 ± 0.03	−2.9 ± 0.1
F15	*−1*	*1*	*0*	*15.0* ± 0.3	0.05 ± 0.001	*−18.0* ± 0.2
F16	0	−1	−1	33.1 ± 0.6	0.21 ± 0.02	−3.1 ± 0.1
F17	−1	−1	0	18.4 ± 0.2	0.04 ± 0.004	−8.6 ± 0.1

Independent Variables	Level used, actual coded		
	−1 (Low)	0 (Medium)	+1 (High)
A: Oil (%)	7.5	10	12.5
B: S_{mix} (%)	25	30	35
C: Water (%)	52.5	60	67.5

solution transparency or turbidity was assessed visually. Ultimately, the pseudo-ternary diagram for the selected composition was constructed through the software CHEMIX School version 12.0 (Arne Standnes, Bergen, Norway).

2.5. Risk assessment

Critical Process Parameters (CPPs) potentially affecting QF-NE-associated Critical Quality Attributes (CQAs) were employed to estimate the risk factors. Risk assessment techniques were used to determine cause-effect relationships between material characteristics and process attributes on the CQAs of the formulation. A Risk Estimate Matrix (REM) was established to find high-risk variables. The REM illustrated the potential risk(s) connected to each material characteristic and method parameter of QF-NE formulations on its potential CQAs by calculating all components' high, medium, or low values. **Table S1** displays the risk analysis for QF- loaded NE formulation; thereby, the high-risk indicators were analyzed using an experimental design.

2.6. QF-NE formulation development

Low-energy emulsification and water titration methodology were employed to design the QF-NE, with the component proportions being determined by the pseudo-ternary phase diagram. Briefly, 100 mg amount of QF was mixed with the Capmul MCM (oil phase) to accomplish complete solubilization. Surfactant and co-surfactant (Tween 20: Transcutol HP) combination were then incorporated into the above drug-oil mixture in a 2:1 ratio to develop a transparent, homogeneous, stable, and homogenous NE (10 mL). Finally, Zetasizer nano ZS (Malvern Instrument, UK) was used to test globule size, uniform size distribution, and zeta potential of the clear or lightly bluish NE).

2.7. Experimental design

Utilizing Design Expert (Ver. 13.0; Stat-Ease Inc., Minneapolis, MN, USA), a Box-Behnken statistical design (BBD) was employed to optimize NE formulations. According to findings obtained by the Design Expert, the Quality by Design (QbD) approach was conducted to optimize the QF-NEs. Notably, the statistical design approach facilitated estimation of the impact of formulation components (oil, S_{mix}, and water) on responses (globule size, PDI, and zeta potential) of NE. To optimize the NEs, the Design Expert offered various theoretical runs with three independent variables and their low (−1), medium (0), and high (+1) levels (Table 1). Eq. (1) depicted the quadratic model formula provided by the software.

$$Y = a_0 + a_1A + a_2B + a_3C + a_{12}AB + a_{13}AC + a_{23}BC + a_{11}A^2 + a_{22}B^2 + a_{33}C^2 \quad (1)$$

where: Y represented the responses, the intercept was represented by a_0, the regression coefficients were represented by a_1 to a_{33}, and the independent variables were depicted by A, B, and C for the Quadratic model.

2.8. Thermodynamic stability of QF-NE formulations

According to the optimization findings, formulation batch F15 exhibited optimum results compared to all other batches (Table 1). Hence, optimized batch F15 was selected for further screenings. Thermodynamic stability for optimized NE formulation was examined by imposing various thermodynamic stresses like freeze–thaw cycles and centrifugation. The centrifugation of NEs was accomplished for 20 min at 10,000 × g, and the formulation was assessed for quality. Simultaneously, NEs were placed for six freeze–thaw cycles at + 40 °C and −20 °C; and were evaluated for stability, including phase separation, globule size, polydispersity, and creaming.

2.9. Development of QF-loaded Chitosan-Poloxamer 407 in-situ gel (QF-Nanoemulgel)

QF-Nanoemulgel formulation was developed upon complete replacement of the water phase with an aqueous in-situ gelling solution of glycol chitosan 1–2 % w/v and poloxamer 407 16–18 % w/v (equivalent to total formulation volume). The aqueous in-situ gelling solution was prepared by dissolving 2 % w/v and 18 % w/v (equivalent to 10 mL of QF-Nanoemulgel) of chitosan and poloxamer in deionized water through gradual stirring. The QF-loaded chitosan and poloxamer 407 in-situ gel was designed upon mixing of aqueous in-situ gelling chitosan and poloxamer 407 solutions in the organic phase containing 7.5 % w/v of oil, 25 % w/v of S_{mix} with continuous stirring at 200 rpm for 30 min. Finally, the developed QF-Nanoemulgel was also tested for further characterization, including thermodynamic stability, (centrifugation and freeze–thaw cycle) globule size, zeta potential, mucoadhesive strength, viscosity, in-vitro release, ex-vivo hemolysis, in-vitro cytotoxicity, and in-vitro cellular uptake and permeation studies.

2.10. Assessment of in-situ gelling

Utilizing a temperature-controlled magnetic stirrer, the sol–gel

transition temperature of the finalized formulation was examined. At a constant temperature increment of 1 °C/min, the mixture swirled at 400 rpm. The temperature at which stirring ceased due to sol–gel transformation, was measured, and recorded.

2.11. Physicochemical characterization for QF nanoformulations

2.11.1. Globule Size, Polydispersity index (PDI), and surface charge (Zeta Potential)

Globule size and size distribution of QF-NE and QF-Nanoemulgel were estimated via the DLS technique employing Zetasizer nano ZS (Malvern Instrument, UK). In addition, PDI was utilized to demonstrate the uniformity of globule size. Besides, the electrical surface charge of nano-globules was also measured by evaluating the zeta potential through Zetasizer nano ZS (Malvern Instrument, UK).

2.11.2. % Transmittance (%T)

The clarity and transparency of developed nanoformulations were screened through UV–visible spectroscopy at a maximum wavelength of 650 nm. Prior to analysis, optimized nanoformulations were diluted with purified water in proportions of 1:1 and 1:5, while purified water was fixed as a blank (Gadhave et al., 2021b).

2.11.3. Drug encapsulation measurement

To measure drug encapsulation, 1 mL of QF-NE and QF-Nanoemulgel formulations incorporating 10 mg/mL of QF (Theoretical drug loading) were centrifuged for 30 min at 10,000 × g at 4 °C. Then, the supernatant was combined with 10 mL of solvent (acetonitrile). Further, a 1:1 ratio of water: acetonitrile (mobile phase) was utilized to prepare the dilution and followed by QF quantification at 294 nm in the supernatants using the UPLC method described in *Section 2.2*. % EE of the nanoparticles were calculated utilizing equations Eq. (2) (Parvathaneni et al., 2021).

$$\%EE = \frac{\text{Weighed QF} - \text{Free QF}}{\text{Weighed QF}} \times 100 \quad (2)$$

$$\text{Hemolysis Ratio}\,(\%) = \frac{\textit{Absorbance of sample} - \textit{Absorbance of control}}{\textit{Absorbance of negative control} - \textit{Absorbance of control}} \times 100 \quad (3)$$

2.11.4. Viscosity and flowability of developed formulations

The viscosity and flowability of QF-NE and QF-Nanoemulgel were analyzed via a Brookfield viscometer (Brookfield Engineering Laboratories Inc., Middleboro, MA, USA), employing spindle 21. Rigorously, 10 mL of the material was examined for viscosity at 25 °C and 34 °C temperatures, while gradually increasing test speed from 5 to 100 rpm. All the measurements were made in triplicate (Gadhave et al., 2023; Kumbhar et al., 2020).

2.11.5. Mucoadhesive potential of developed QF-Nanoemulgel

QF-NE and QF-Nanoemulgel were assessed for mucoadhesion and consistency, utilizing a texture analyzer (TA.XT Plus, Hamilton, MA., USA). During the experiment, a cylindrical probe was dipped in the formulation for 10 sec after applying it to freshly collected rat nasal epithelial mucosa (obtained from the animal care center at St. John's University). Measurements were completed at a 1 mm/sec speed with a 3 g of trigger force. Finally, the force required to detach the contact of gel and mucosa was confirmed and reported. (Chatzitaki et al., 2020; Gadhave et al., 2019a; Kumbhar et al., 2021).

2.11.6. In-vitro QF release study

In-vitro release of QF from developed NE and Nanoemulgel were performed in simulated nasal electrolyte solution (SNES, pH 6.4), using the 0.1–0.5 mL dialysis cassettes (2,000 MWCO, Thermo Scientific, Waltham, MA, USA). SNES was prepared by following the protocol as described by (Gadhave and Kokare, 2019; Kokare et al., 2020). Briefly, the dialysis cassettes were placed in SNES (pH 6.4) to equilibrate for 10 min. Then, 500 µL of the formulation was loaded into the hydrated cassette membrane, which were then submerged into a beaker containing 100 mL of SNES (pH 6.4; 34 ± 0.5 °C) and stirred for 200 rpm. Subsequently, 1 mL of samples were collected and replenished with fresh SNES at predetermined intervals, i.e., 0.5, 1, 2, 4, 8, 12, and 24 h. The above samples were diluted by mobile phase and then analyzed via the validated UPLC method as described earlier.

2.11.7. Ex-vivo hemolysis study

According to previously published reports, long-term therapy with QF induced hemolytic anemia in individuals. Thereby, the following formulations, i.e., distilled water (control), 0.01 % sodium lauryl sulfate, QF, QF-NE, and QF-Nanoemulgel (10, 50, and 100 µg/mL) were screened for hemolysis. For this study, 4 mL of blood samples were collected from male Sprague-Dawley rats (175–200 g; to be euthanized, St. John's animal facility) utilizing a 23-gauge needle from the lateral saphenous vein in heparinized blood collection tubes. Subsequently, these blood samples were centrifuged at 3,000 × g for 10 min. Simultaneously, the plasma was withdrawn, erythrocytes were rinsed thrice with saline water, and were incubated with predefined concentrations (10, 50, and 100 µg/mL) of formulations and controls at 37 °C. Then the samples (200 µL each) were collected at different intervals, i.e., 0.5, 4, and 10 h. Further, these samples were centrifuged at 13,000 × g for 10 min. Ultimately, the samples were screened under a microscope, and the absorbance was measured at 570 nm with Spark 10 M Plate Reader (Tecan, Männedorf, Switzerland). The equation (Eq. (3) was utilized to estimate the hemolysis percentage (Godara et al., 2020; Jeswani et al., 2021; Van De Ven et al., 2012).

2.11.8. Stability evaluation

According to ICH guidelines (Q1a(R_2)), the shelf-life of developed QF-NE and QF-Nanoemulgel were tested using accelerated stability conditions. Formulations were placed in a stability chamber (VWR™ stability chamber, Radnor, PA, USA) at 40 °C/75 % RH for three months. The samples were tested after three months for important physicochemical characteristics such as QF content, globule size, PDI, % transmittance, and zeta potential (Chatzitaki et al., 2020).

2.12. Cell culture studies

For the cell culture studies, RPMI-2650 human nasal epithelial cell lines (ATCC; Manassas, VA, USA) were cultured utilizing EMEM cell growth media augmented with 1 % antibiotics (penicillin–streptomycin) and 10 % Fetal Bovine Serum (FBS). Cells were incubated to 85–90 % confluency in 5 % CO_2 at 37 °C. Subsequently, confluent cells were trypsinized and used for different studies, such as qualitative and quantitative cellular uptake, cell viability, and cell permeability studies (Gonçalves et al., 2016; Parvathaneni et al., 2021; Wang et al., 2020).

2.12.1. In-vitro cell viability

Briefly, 2,500 cells/well were plated in 96-well TC-treated plates and were incubated overnight under essential conditions for complete

adherence. On the next day, the cells were treated with different concentrations of pure QF, Blank-Nanoemulgel, and QF-Nanoemulgel (equivalent to 0.78125–25 μM of QF), and blank media treated cells were used as control. Following 4, 12, and 24 h incubation, the cell viability was quantified by MTT assay, as described earlier (Parvathaneni et al., 2020; Vaidya et al., 2019). Eq. (4) and Eq. (5) were used to calculate the % vitality of RPMI-2650 cells (Chatzitaki et al., 2020; Parvathaneni et al., 2020).

$$\text{Cell viability}\ (\%) = \frac{\text{Mean absorbance of treatment}}{\text{Mean absorbance of control}} \times 100 \quad (4)$$

$$Inhibitingcells(\%) = 100 - viablecells \quad (5)$$

2.12.2. Cellular uptake by fluorescence microscopy

A cellular uptake experiment was accomplished to determine the effect of drug encapsulation in developed Nanoemulgel formulation on intracellular uptake, by using a fluorescent dye, coumarin-6. Nanoemulgel was prepared with 1 mg/mL fluorescent dye (coumarin-6) for cellular uptake. Detailed procedure is outlined in *Supplementary Material*.

2.12.3. Quantification of Nanoemulgel mediated intracellular uptake of Coumarin-6

To quantify the intracellular uptake of coumarin-6 and coumarin-6-Nanoemulgel formulations in RPMI-2650, we used Nexcelom Cellometer Vision (Nexcelom, Lawrence, MA, USA). The RPMI-2650 cells were seeded overnight into a TC-treated cell culture petri dish, 150 MM (5×10^6 cells/sterile petri dish), and on the next day, treated with coumarin-6 (1 μg/mL) and coumarin-6-Nanoemulgel (1 μg/mL) for 3 h before the analysis. After being trypsinized, the cells were centrifuged at 1,957 × g and rewashed with ice-cold PBS. Then the collected pellets were dispersed in 50 μL of PBS, and a Nexcelom Cellometer Vision fluorescent cell counter was used to assess the amount of coumarin-6 cellular uptake. The mean fluorescence intensity (MFI) of the coumarin-6 solution and coumarin-6-Nanoemulgel were then compared with control RPMI-2650 cells (Alqahtani et al., 2015; K Shukla et al., 2022; Vaidya et al., 2020).

2.12.4. Drug transport and permeation studies across RPMI-2650 monolayers

RPMI-2650 monolayers have been widely utilized to assess the drug transport and permeation across the nasal epithelial barrier (Gonçalves et al., 2016; Sibinovska et al., 2019). For our studies, we developed RPMI-2650 monolayers by seeding the cell on polyester Transwell™ inserts (12-well plates, area 0.33 cm^2, 0.4 μm pore size). Exactly 100 μL of cell suspension was seeded at 8.5×10^4 cells/ insert to create the air–liquid interface (ALI) model. Finally, plates were incubated at 37 °C/ 5% CO_2, and 95 % air humidity. Monolayer formation was determined by timely measurement of *trans*-epithelial electrical resistance (TEER) (Ladel et al., 2019; Vaz et al., 2022).

2.12.5. Trans-epithelial electrical resistance (TEER) measurements

The integrity of cell monolayer was assessed utilizing TEER testing. This non-invasive and safe approach reflects ionic resistance across the cell layer during various development and differentiation stages. The TEER values of RPMI-2650 cultures were assessed every 2 to 3 days to ensure appropriate cell growth during incubation, using an EVOM® resistance meter and Endohm® chamber (World Precision Instruments, Sarasota, FL, USA) (Vaz et al., 2022). For this experiment, after 16 days, a TEER value of approximately 80 Ωcm^2 was required to obtain a complete monolayer. As the size and density of the pores on the insert membrane affect the TEER value, the measurement strategy includes estimating the blank resistance (R_{Blank}) of the membrane (without cells) and the resistance over the cell layer on the insert membrane (R_{Total}). The following formulas were used to calculate the final cell membrane resistance.

$$R_{Cells(\Omega)} = R_{Total} - R_{Blank} \quad (6)$$

$$TEER_{Cells} = R_{Cells(\Omega)} \times M_{Area(cm^2)} \quad (7)$$

2.12.6. QF permeation across RPMI-2650 cells

Once TEER values stabilized within 75–85 Ωcm^2 (signifying formation of monolayers, after 16 days in this case), the permeation potential of developed QF solution and QF-Nanoemulgel formulations were determined across RPMI-2650 cell epithelial monolayer after 3 h of treatment. The apical chamber (donor) of the Transwell™ insert was filled with 100 μL of the formulation. Simultaneously, the Transwell™ basal chamber (acceptor) medium was filled with 600 μL of fresh EMEM media. After adding QF solution and QF-Nanoemulgel (12.5 and 25 μM of QF), plates were incubated at 37 °C/5% CO_2. Exactly 100 μL of the medium was withdrawn from the acceptor compartment once per h for up to 3 h, and again the same volume of fresh media was refilled to maintain the volume of the acceptor chamber. After completion of the experiment, all samples were analyzed via validated UV spectrophotometer method for QF content in triplicate, EMEM media was used as a blank for analysis (Gonçalves et al., 2016).

2.13. Statistical analysis & Data representation

The statistical analysis was carried out using GraphPad Prism 9.0 software. Every experiment was conducted at least in triplicate (n = 6 in each trial for cell culture studies), and data were represented as mean ± SD. Experimental outcomes were estimated utilizing the student's *t*-test while comparing unpaired samples from two groups. The cytotoxicity, uptake, and permeation study outcomes were analyzed through Tukey's post-hoc comparison with ANOVA, and the p-value (*p < *0.05*) was statistically significant.

3. Results and discussion

Therapeutic applications of existing antipsychotics are associated with several life-threatening effects, especially thrombocytopenia, hemolytic anemia, leukopenia, and agranulocytosis, etc. Many of the current antipsychotic medications exhibit poor solubility, oral absorption, and bioavailability, which results in limited use, and high dose requirement for therapeutic benefits. In the current work, an attempt was made to develop a quetiapine (QF)-Nanoemulgel formulation, which may help to overcome the earlier limitations by reducing peripheral exposure and facilitating direct transport to the brain. The nose-to-brain drug delivery approach is based on two crucial physicochemical characteristics of the drug, i.e., molecular weight and lipophilicity. QF is a BCS class-II molecule with an appropriate molecular mass (441.5 g/mol) and higher lipophilicity (Log $p > 2.8$), which makes it very suitable for nose-to-brain delivery.

3.1. Developmental approach of QF-loaded nanoformulations

Screening components for nanoformulation is a crucial step implemented during the pre-formulation studies. For developing a novel drug delivery approach, excipients were selected based on the solubility of QF in numerous GRAS (Generally Recognized as Safe)-designated excipients. As a result of saturation solubility, the excessive solubility of QF was revealed in Capmul MCM among the oils, which was fixed as the oil phase for NE. In addition, Transcutol HP and Tween 20 were selected as co-surfactant and surfactant, respectively. Tween 20, a non-ionic surfactant, is preferred as a safe ingredient for human consumption, and possesses an excellent HLB value of around 16.7. These properties make Tween 20 highly applicable in nanoparticulate drug delivery systems to improve the permeability of drugs across physiological barriers (BBB). At the same time, Transcutol HP is a generally used component in

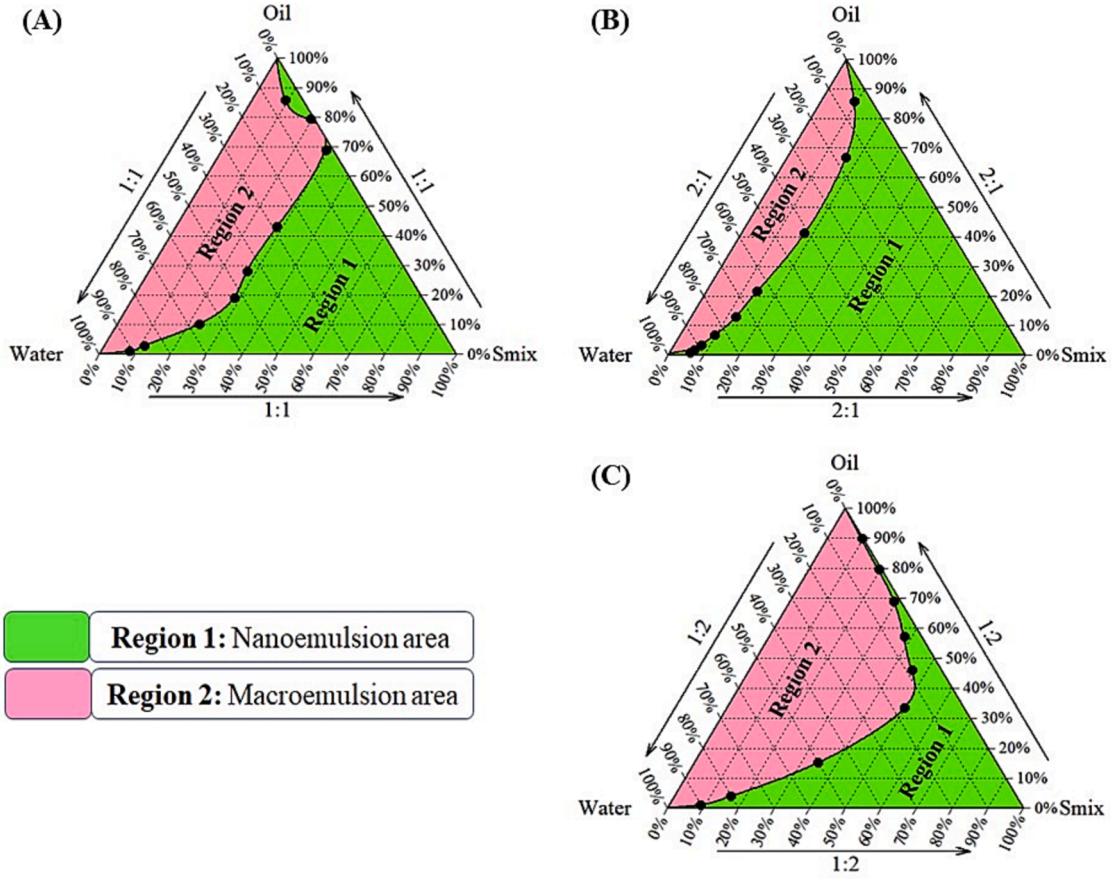

Fig. 1. Preformulation studies for development of QF nanoformulations: pseudo-ternary phase diagrams of S_{mix} ratios **(A)** 1:1, **(B)** 2:1, and **(C)** 1:2.

pharmaceutical products, which is known to be devoid of chronic, subchronic toxicity, and genotoxicity, as evidenced by available reports. Therefore, selected ingredients were preferred as safe for developing a QF-loaded NE system.

The NE regions were assessed from the pseudo-ternary phase diagrams in the subsequent NE development stage. Drug penetration from the hydrophobic region of the surfactant molecule into the oil phase is essential to enhance the NE fluidity. This phenomenon helps to lower the interfacial tension between the aqueous and oil phases. Thereby, the co-surfactant helps to increase the formulation's fluidity to construct an appropriate surfactant coat over the oil globules. In this context, surfactants and co-surfactants (S_{mix}) were employed in various proportions, like 1:1 **(**Fig. 1**A)**, 2:1 **(**Fig. 1**B)**, and 1:2 **(**Fig. 1**C)**, and the phase diagram was constructed. In contrast, these diagrams help to suggest the excessive NE region. The graph was designed through CHEMIX school (12.0) software, and the maximum NE region (Region 1) was reflected at a 2:1 ratio of surfactant: co-surfactant combination (Fig. 1B). Hence, the 2:1 S_{mix} ratio was employed to develop the uniform, clear, and stable NE formulation while compared with other ratios. Consequently, a 2:1 S_{mix} ratio was employed to formulate a stable QF-loaded NE nanosystem.

3.2. Optimization of QF-loaded NE

The technique outlined in the methodology section was used to construct the seventeen QF-NE formulations (F1-F17; Table 1**)**, which helped determine the interaction of formulation variables on globule size, PDI, and zeta potential. Various test batches of QF-NEs were designed by blending 7.5–12.5 % of the oil phase (Capmul MCM), 20–25 % of S_{mix} (Tween 20: Transcutol HP at 2:1 ratio), and 62.5 % of water, through aqueous titration method with continuous stirring. The observed values for responses, such as globule size (Y_1), PDI (Y_2), and zeta potential (Y_3), were revealed to be in close agreement with predicted values. Additionally, Table S2 depicts the statistical outcome of the interaction between the oil phase, S_{mix}, and aqueous phase, on globule size. The quadratic model is significant for all three dependent variables; according to the model, *p*-values for globule size, PDI, and zeta potential were 0.0001, 0.0003, and 0.0003, respectively, for the quadratic model. The interaction of Model term A (changes in % of oil) has exhibited a significant impact **(**$*p < 0.05$**)** on all the dependent variables. In contrast, the model terms B and C displayed non-significant influence. Hence, the quadratic model has been further used to explore the design space. Besides, the significant influence of model term A on all responses was supported by the highest coefficient values of model term A for globule size (+22.8 nm), PDI (+0.0592), and zeta potential (–5.54 mV) in the developed polynomial equations on the interaction of formulation factors on globule size (Eq. (8), PDI (Eq. (9) and zeta potential (Eq. (10).

$$Globulesize(Y_1) = +22.80 + 31.92*A - 8.74*B - 4.23*C - 8.35*AB - 4.27*AC + 0.3050*BC + 22.09*A^2 + 0.0685*B^2 + 1.55*C^2 \quad (8)$$

$$Polydispersityindex(Y_2) = +0.0592 + 0.1265*A - 0.0730*B - 0.0223*C - 0.1073*AB - 0.0048*AC + 0.0367*BC + 0.0955*A^2 + 0.0215*B^2 + 0.0170*C^2 \quad (9)$$

$$Zetapotential(Y_3) = -5.45 + 3.12*A - 1.12*B - 0.3350*C - 0.0925*AB + 0.1525*AC - 0.2725*BC - 1.66*A^2 + 0.2082*B^2 + 0.3183*C^2 \quad (10)$$

Further, the maximum coefficient values of model term A in Eq. (9), 10, and 11 meet with the 3D surface plots (Fig. 2A and 2B). The unfavorable coefficient value of A on globule size and PDI demonstrated that increasing oil concentration increases globule size and PDI values. Furthermore, the increase in size and PDI depicts the decrease in zeta

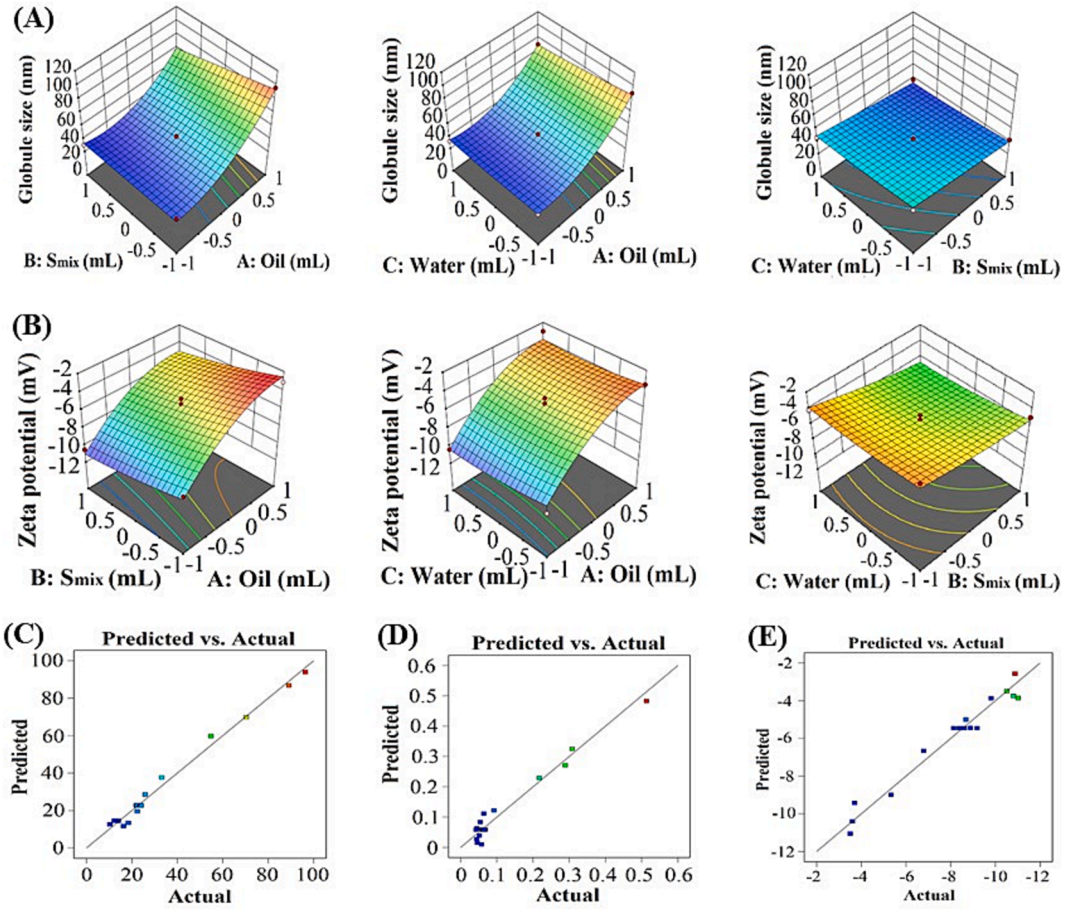

Fig. 2. Three-dimensional response surface plots for the effect of formulation variables on **(A)** globule size, **(B)** zeta potential. Linear correlation plots between the actual and predicted values for **(C)** globule size, **(D)** PDI and **(E)** zeta potential.

Table 2
Observations for thermodynamic stability of QF-NE and QF-Nanoemulgel after centrifugation and freeze–thaw cycle.

Parameters	QF-NE		QF-Nanoemulgel	
	Centrifugation	Freeze-thaw cycles	Centrifugation	Freeze-thaw cycles
Globule size (nm)	15.1 ± 0.7	15.9 ± 0.5	19.9 ± 0.8	20.3 ± 0.4
Zeta potential	−18.4 ± 0.3	−17.7 ± 0.9	+20.2 ± 0.4	+19.7 ± 0.2
PDI	0.05 ± 0.001	0.09 ± 0.005	0.126 ± 0.02	0.201 ± 0.05
% Transmittance	99.5 ± 0.4	99.3 ± 0.7	99.0 ± 1.1	98.5 ± 1.3
Phase separation	No	No	No	No
Creaming	No	No	No	No

QF-NE: *Quetiapine hemifumarate nanoemulsion;* QF-Nanoemulgel: *Quetiapine hemifumarate Nanoemulgel;* PDI: *Polydispersity index*.

potential. Thus, it described a rise in oil % that could increase the globule size and PDI of the NE system, which coordinates with the positive coefficient value (+31.92 and + 0.126) of model term A in Eq. (9) and (10). The larger size particles retarded the QF permeation and absorption, leading to loss of medication from the site of administration. However, the percentage error was < 5 %, indicating that the experimental and predicted values were closely matched **(**Fig. 2**C-E)**. % error helped to assess the accuracy of software-created equations. Optimized F15 NE formulation composed with oil (7.5 %), S_{mix} (25 %), and water (67.5 %), and this mixture met the optimum requirements for nanoscale globule size (15.0 ± 0.4 nm), PDI (0.054 ± 0.001), and zeta potential (-18.0 ± 0.6 mV). As a result, all responses were perfectly correlated with the F15 NE system, and this formulation was chosen for further research.

3.3. Thermodynamic stability of QF-NE formulations

Further, the optimized NE was investigated for thermodynamic stability through centrifugation and freeze–thaw cycle. Outcomes revealed that the centrifugation and freeze–thaw examinations showed no signs of phase separation, creaming, sedimentation, and drug precipitation (Table 2). That confirmed the QF-NE exhibited higher stability after centrifugation at 10000 × g for 20 min. Simultaneously, it demonstrated excellent potency against freeze–thaw cycles, proving the developed QF-NE was thermodynamically stable.

3.4. Preparation of in-situ gel formulation

The present research intended to extend the intranasal localization time of the developed nanoformulation to properly transport the incorporated medicine in the brain. Various in-situ gelling agents were

Table 3
Final composition of QF-NE and QF-Nanoemulgel formulation (QF-Nanoemulgel formulation contained blend of 2 % w/v and 18 % w/v (equivalent to 10 mL of Nanoemulgel) of chitosan and poloxamer 407, respectively, in water).

Category	Name of component	Optimized QF-NE composition	Optimized QF-Nanoemulgel composition
Oil	Capmul MCM	7.5 % w/v	7.5 % w/v
Surfactant	Tween 20	16.6 % w/v	16.6 % w/v
Cosurfactant	Transcutol HP	8.3 % w/v	8.3 % w/v
Aqueous phase (q. s.)	Water	67.5 % w/v	47.5 % w/v
Natural mucoadhesive agent	Chitosan	–	2 % w/v
In-situ gelling agent	Poloxamer 407	–	18 % w/v

Each QF-NE formulation contains QF 10 mg/mL, each optimized QF-Nanoemulgel formulation contains QF 10 mg/mL.

scanned during the experiment to establish mucoadhesive formulation. The gelation potency of multiple polymers, i.e., chitosan, HPMC K4M, poloxamer 407, and carbopol 974P etc., were evaluated for their gelling features. In-vitro, the combination of chitosan (2 %) and poloxamer 407 (18 %) formed a thermosensitive gel with the proper consistency. However, HPMC K4M (0.5 %) and carbopol 974P (0.5 %) produced a highly rigid gel at a physiological pH. Likewise, poloxamer 407 and chitosan had a stable gel for intranasal administration at 34 ± 0.5 °C, while other polymers developed unstable gels. Therefore, 2 % chitosan and 18 % poloxamer 407 formed a stable and suitable in-situ mucoadhesive gelling system (Table 3). The final optimized QF-Nanoemulgel formulation was then tested for thermodynamic stability and the results proved excellent stability (Table 2).

3.5. Physicochemical characterization of QF-loaded nanoformulations

3.5.1. Analysis of globule Size, PDI and zeta potential

The size of the dispersed nano globules in the fabricated NE system reflects the globule size measurement, Fig. 3**A** depicts the optimized physicochemical parameters for NE and Nanoemulgel formulation. Optimized QF-NE and QF-Nanoemulgel formulations evaluated for globule size were 15.0 ± 0.3 nm and 20.4 ± 0.7 nm, respectively (Fig. S1**A & S1B**). The nanosized particles with a large surface area are instrumental in circumventing the BBB via the IN route and efficiently deliver medicine into the CNS. Polydispersity index (PDI) analysis was used to examine the uniform distribution of nanoparticles. PDI for optimized QF-NE and QF-Nanoemulgel were depicted as 0.05 ± 0.001 and 0.121 ± 0.01 (Fig. 3**A**), respectively, within a limit of <1. Thereby, outcomes demonstrated that the uniform distribution of globules in the NE system helps diminish the possibilities of particle aggregation. Fig. 3**A** represented the optimized zeta potential for QF-NE and QF-Nanoemulgel and was reported as −18.3 ± 0.2 mV and +21.5 ± 0.9 mV, whereas Fig. S1**C & S1D** reflected the diagrammatic representation of zeta potential for NE and Nanoemulgel. The anionic surface charge increases the stability of NE due to the repulsion of like-charged particles and may decrease the force of particle aggregation (Kokare et al., 2020; Shah et al., 2016). The chitosan/poloxamer 407 loaded NE formulation demonstrated a positive charge due to the coating of cationic ingredients on the NE system, resulting in ionic interchange between the cationic charge of the chitosan-poloxamer-coated NE. Further, the carboxy group of cationic polymers interacting with mucin helps enhance the mucoadhesion of the Nanoemulgel formulation (Vaidya et al., 2020; Wilson et al., 2021).

3.5.2. % Transmittance (%T) measurement

Transparency and optical clarity of the proposed nanoformulation

(A)

Formulations	Physicochemical characterization			
	Globule size (nm)	Polydispersity Index	Zeta potential (mV)	Transmittance (%)
QF-NE	15.0 ± 0.3	0.05 ± 0.001	−18.3 ± 0.2	99.6 ± 0.4
QF-Nanoemulgel	20.4 ± 0.7	0.121 ± 0.01	+21.5 ± 0.9	98.5 ± 1.2

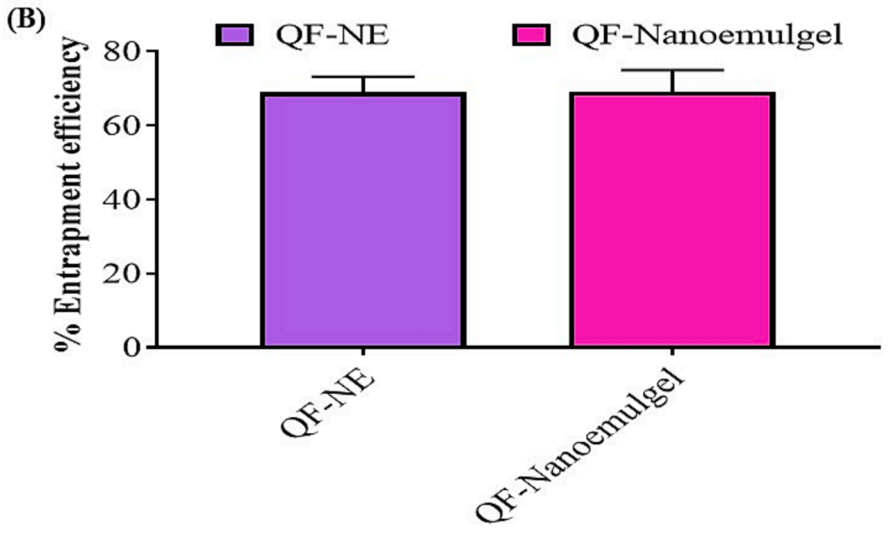

Fig. 3. Physico-chemical characterization of developed nanoformulations: **(A)** globule size, PDI, zeta potential and % T of QF-NE, and QF-Nanoemulgel. **(B)** Analysis of QF % entrapment efficiency in QF-NE and QF-Nanoemulgel. Values are represented as the mean ± SD ($n = 3$), $^{*}p < 0.05$.

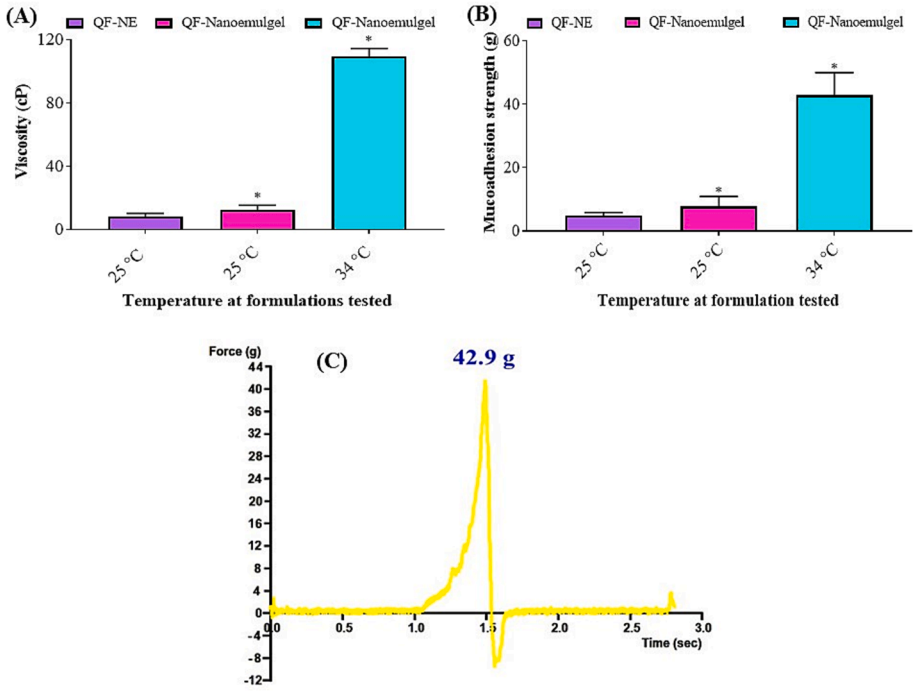

Fig. 4. **(A)** Determination of viscosity, **(B)** *ex-vivo* mucoadhesive strength of QF-NE and QF-Nanoemulgel formulations and **(C)** representative image for mucoadhesive strength of QF-Nanoemulgel at 34 °C. Values are represented as the mean ± SD ($n = 3$), $^{*}p < 0.05$ corresponding to QF-Nanoemulgel formulation.

were investigated using a % transmittance study, which helps to confirm the stability of developed nanoformulations. Transmittance for QF-NE and QF-Nanoemulgel was obtained as 99.6 ± 0.4 % and 98.5 ± 1.2 %, respectively. QF-NE appeared transparent with a bluish tint, while QF-Nanoemulgel seemed clear (Fig. 3**A**). Finally, the outcomes of the transmittance study revealed the clarity and transparency of the nanoformulations, which supported the previous findings (Alaayedi and Maraie, 2023; Tarik Alhamdany et al., 2021).

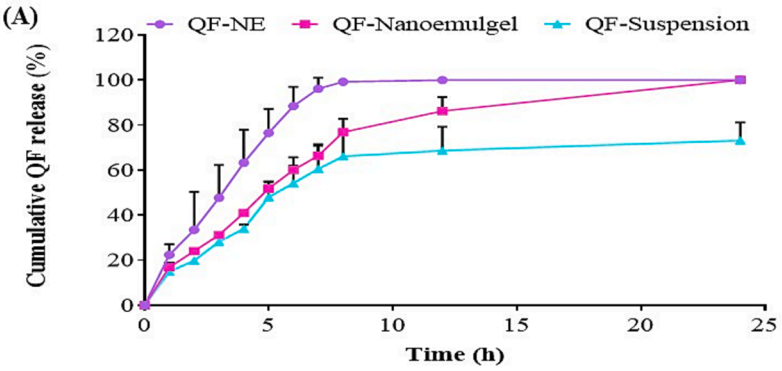

(B)

Release kinetic models	Formulations		
	QF-NE (R^2)	QF-Nanoemulgel (R^2)	QF-Suspension (R^2)
Zero-order	0.993	0.989	0.983
First-order	0.937	0.983	0.972
Higuchi	0.946	0.947	0.926
Hixon-Crowel cube root	0.977	0.98	0.987
Korsmeyer-Peppas	0.938	0.916	0.903
n = Release exponent	(n = 0.755)	(n = 0.705)	(n = 0.725)

QF-NE: Quetiapine hemifumarate nanoemulsion, *QF-Nanoemulgel:* Quetiapine hemifumarate chitosan poloxamer nanoemulgel, R^2: Regression coefficient

Fig. 5. **(A)** Cumulative QF release from QF-Suspension, QF-NE and QF-Nanoemulgel over 24 h via a dialysis cassette. (B) The regression coefficient of kinetic models observed for QF-loaded formulations.

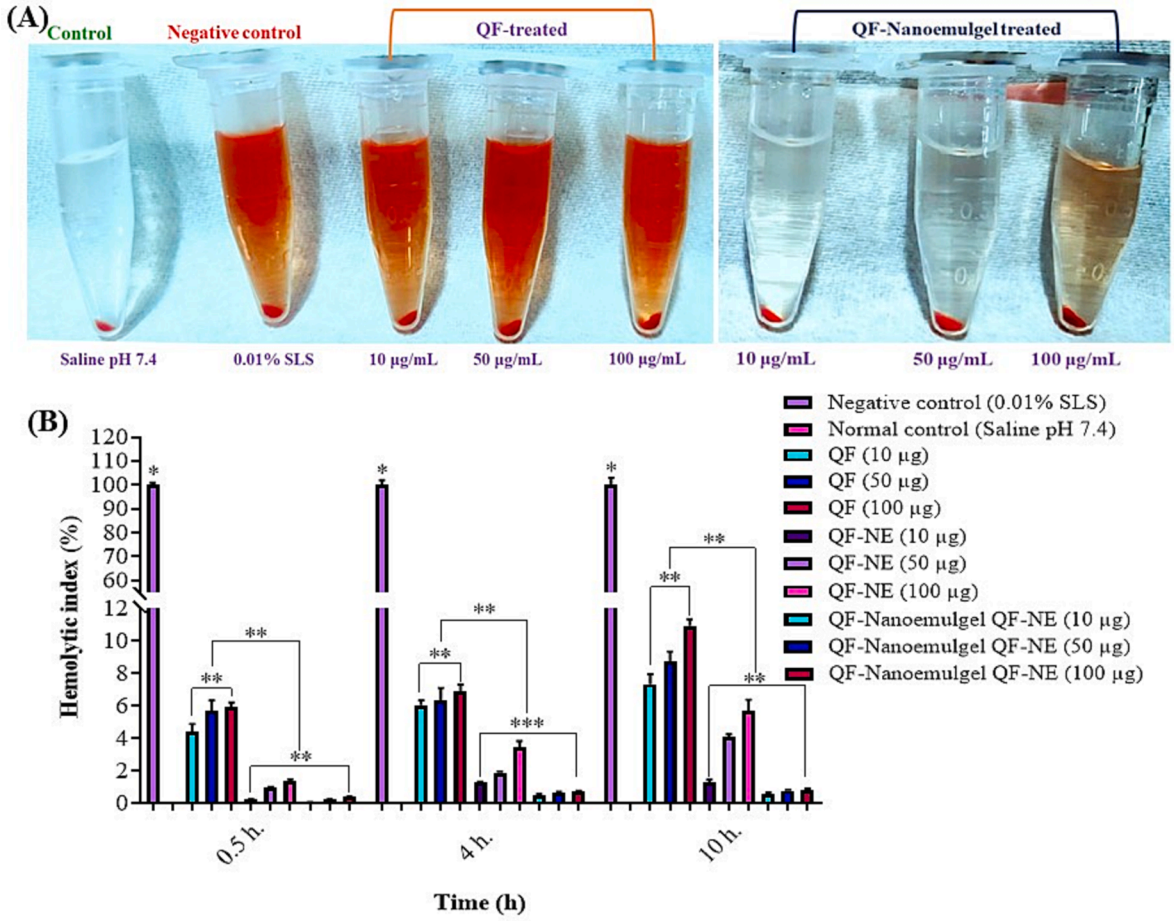

Fig. 6. (A) Visual examination of the blood samples treated with 10, 50 and 100 µg/mL of pure QF, QF-NE and QF-Nanoemulgel formulation against 0.01 % of negative control (SLS) in the microcentrifuge tubes and (B) % hemolysis (hemolytic index) caused by pure QF, QF-NE and QF-Nanoemulgel at different concentrations (10, 50 and 100 µg/mL) against negative control. Data expressed as mean ± SD ($n = 3$). *$p < 0.05$, **$p < 0.01$, ***$p < 0.005$.

3.5.3. *Entrapment efficiency of QF nanoformulations*

QF encapsulation efficiency is one of the most important criteria in evaluating the drug loading strength at the selected co-surfactant and surfactant concentrations. The encapsulation and loading potential for developed QF-NE and QF-Nanoemulgel are illustrated in Fig. 3**B**. Outcomes demonstrated that the drug encapsulation efficiencies of QF-NE and QF-Nanoemulgel were depicted at 69.0 ± 2.2 % and 69.2 ± 1.8 %, respectively, resulting in a drug concentration of 6.9 ± 0.2 mg/mL and 6.92 ± 0.1 mg/mL, respectively. Ideal drug entrapment of NE and Nanoemulgel demonstrated their suitability with selected oils, surfactants, and co-surfactants. The excellent drug entrapment potential of NE and Nanoemulgel formulations makes them ideal carriers for QF delivery to the brain.

3.5.4. *Viscosity analysis of Nanoemulgel formulation*

In this analysis, the QF-NE demonstrated lower viscosity (8.4 ± 0.2 cP), which confirmed outstanding fluidity and ease of nasal installation (Fig. 4A). In contrast, QF-Nanoemulgel (12.5 ± 0.9 cP) was slightly denser than QF-NE, possibly due to mucoadhesive and gelling polymers, but it was still deemed feasible for nasal application. However, the viscosity of QF-Nanoemulgel at the nasal temperature was enhanced up to 109.5 ± 1.5 cP, a 9–10-fold increase compared to room temperature (Fig. 4A). Findings suggest that the chitosan and poloxamer *in-situ* gelling polymers could boost the viscosity of QF-Nanoemulgel following IN administration; hence, it helps to overcome the hurdle of mucociliary clearance (Cho et al., 2011; Gadhave et al., 2021a; Mura et al., 2018; Radivojša et al., 2013).

3.5.5. *Ex-vivo mucoadhesion potential*

The respiratory system's defensive mechanism, mucociliary clearance, shields the nasal cavity from external hazards and pathogens. Consequently, the liquid formulations are rapidly removed from the nose after application. However, improper localization time is the biggest obstacle to therapeutic drug absorption via the IN route. Compared to the mucoadhesive force (7.8 ± 0.4 g) of QF-Nanoemulgel, QF-NE exhibited a lower mucoadhesive strength (4.8 ± 0.2 g) to detach the bonds between formulations and the mucosa at the ambient temperature (25 ± 0.5 °C), thus indicating maximum fluidity and less viscosity. However, QF-Nanoemulgel exhibited significantly higher mucoadhesive strength, around 42.9 ± 1.9 g at intranasal physiological temperature (34 ± 0.5 °C), possibly due to the polymer's thermosensitive nature. Fig. 4**B** depicts the mucoadhesive strength of developed QF-NE and QF-Nanoemulgel formulations and reveals that higher mucoadhesion at nasal temperature could enhance the localization time. Fig. 4**C** presents a representative histogram of mucoadhesion measurement for QF-Nanoemulgel at physiological temperature. The results suggest that the newly developed QF-Nanoemulgel may aid in overcoming the limitations imposed by mucociliary clearance and improve the delivery of medication to the site of action (Kumbhar et al., 2020; Pathak et al., 2014; Vaz et al., 2022).

3.5.6. *In-vitro QF release study*

The drug release form developed QF-NE and Nanoemulgel formulations were compared with QF-Suspension. In contrast to release from QF-NE and QF-Suspension, which demonstrated 99.2 ± 0.6 % and 66.1 ± 1.6

Table 4
Stability evaluation of QF-NE and QF-Nanoemulgel for 3 months.

Formulations	Parameters	Time			
		Initial	1 month	2 months	3 months
QF-NE	Particle size* (nm)	15.3 ± 0.4	15.6 ± 0.7	16.4 ± 0.4	16.8 ± 0.5
QF-Nanoemulgel		20.4 ± 0.3	20.8 ± 0.2	21.4 ± 0.6	22.4 ± 0.4
QF-NE	PDI*	0.05 ± 0.002	0.07 ± 0.004	0.07 ± 0.005	0.09 ± 0.003
QF-Nanoemulgel		0.121 ± 0.01	0.144 ± 0.03	0.239 ± 0.01	0.246 ± 0.02
QF-NE	ζ-potential* (mV)	−18.3 ± 0.4	−17.5 ± 0.3	−17.8 ± 0.2	−16.4 ± 0.3
QF-Nanoemulgel		+21.5 ± 0.4	+20.9 ± 0.5	+20.6 ± 0.6	+20.2 ± 0.3
QF-NE	Transmittance (%)	99.6 ± 0.4	99.2 ± 0.7	99.4 ± 0.5	99.0 ± 1.1
QF-Nanoemulgel		98.5 ± 1.4	98.2 ± 1.8	98.5 ± 1.5	98.2 ± 1.8
QF-NE	Entrapment efficiency (%)	69.0 ± 2.1	68.7 ± 1.4	68.6 ± 1.2	68.5 ± 1.8
QF-Nanoemulgel		69.2 ± 2.3	69.1 ± 1.9	69.0 ± 2.6	69.0 ± 1.6

QF-NE: Quetiapine hemifumarate nanoemulsion; QF-Nanoemulgel: Quetiapine hemifumarate Nanoemulgel; PDI: Polydispersity index.

% cumulative release, respectively in 8 h, the cumulative release of QF from the fabricated QF-Nanoemulgel was 77.0 ± 2.7 % after 8 h (Fig. 5A). The experimental findings demonstrated that the QF-NE released more quickly than the QF-Nanoemulgel. The prolonged release of QF from the QF-Nanoemulgel formulation could be due to the mucoadhesive/gelling polymers, which potentially controlled the drug's permeation rate, leading to a sustained release. The rapid release of QF from QF-NE occurred due to nano globule size, which supports the higher surface area and could quickly release across the dialysis membrane (Choudhury et al., 2019; Gadhave et al., 2022; Kumbhar et al., 2020). The globule size of QF-NE and QF-Nanoemulgel was < 20 nm, contributing to QF's enhanced solubility. Further, inadequate solubility of QF in QF-Suspension can cause poor drug release, where the coarse particles in suspension retard the rate of QF release through the dialysis membrane. Subsequently, the release pattern was analyzed through release kinetic models, and the zero-order kinetic model emerged as the best-fit model based on the regression coefficient (R^2), which was found to be 0.993 and 0.989 for QF-NE and QF-Nanoemulgel, respectively (Fig. 5B). The plotted release kinetic models for QF-NE and QF-Nanoemulgel formulations are depicted in **Fig. S2**. The Zero-order kinetics model exhibits controlled QF release irrespective of SNES fluid concentration until the system is saturated. In contrast, QF-Nanoemulgel reveals a sustained release for 24 h compared to QF-NE and QF-Suspension. Simultaneously, zero-order kinetics supported the constant amount of drug eliminated per unit of time. Additionally, the sustained/controlled release of QF from the QF-Nanoemulgel is more feasible for extended absorption through IN route than other formulations (*p < 0.05).

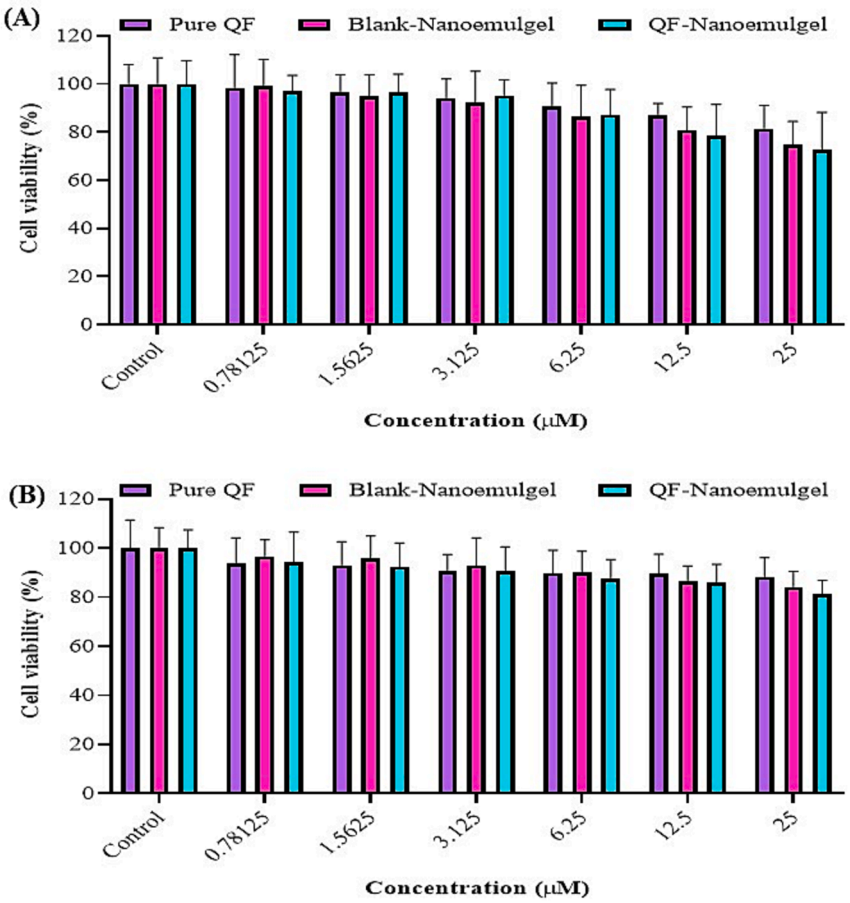

Fig. 7. MTT assay and cell viability comparison for pure QF, Blank-Nanoemulgel and QF-Nanoemulgel formulations on human nasal epithelial RPMI-2650 after **(A)** 24 h and **(B)** 12 h treatments. All values are expressed as mean ± SD (n = 3), *$p < 0.05$.

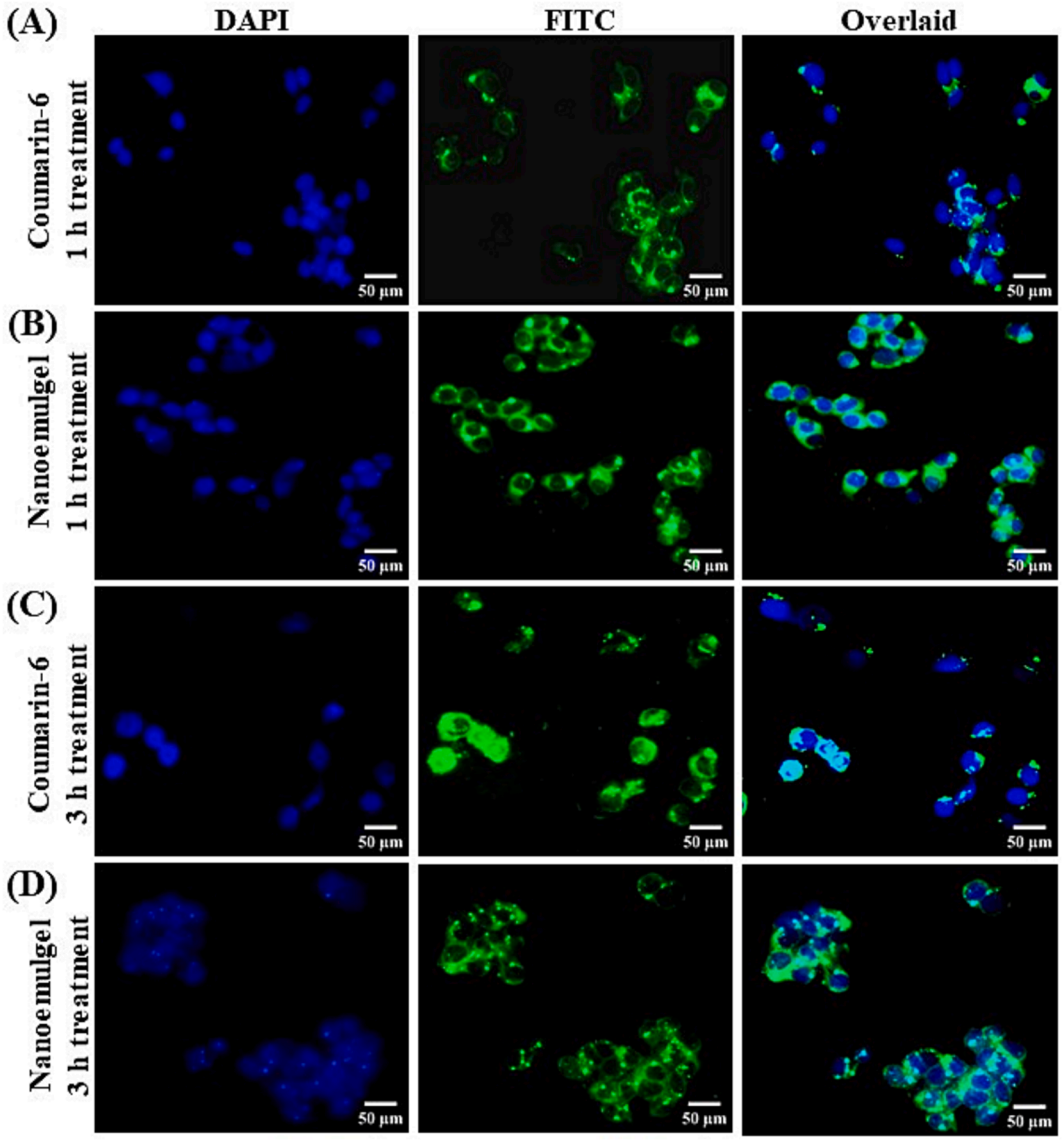

Fig. 8. In-vitro cellular uptake of coumarin-6 (control) and coumarin-6-loaded Nanoemulgel in RPMI-2650 cells. Fluorescence microscopy images: **(A)** control treated cells for 1 h (Nuclei are stained blue with DAPI and coumarin-6/coumarin-6-Nanoemulgel are stained green), **(B)** coumarin-6-Nanoemulgel treated cells for 1 h, **(C)** control treated cells for 3 h and **(D)** coumarin-6-Nanoemulgel treated cells for 3 h. Scale bar = 50 µm.

3.5.7. Ex-vivo hemolysis study

Hemolysis is a complicated process in which red blood cells (RBCs) rupture and break; to evaluate the hemolytic effect of developed QF-NE and QF-Nanoemulgel, we determined the amount of hemoglobin released after erythrocyte destruction. An erythrocyte suspension made from freshly drawn rat whole blood in normal saline was used to assess the hemolytic activity of QF-Suspension, QF-NE, and QF-Nanoemulgel. After incubation for 30 min, red blood cell suspensions were treated with various concentrations of QF-Suspension, QF-NE, and QF-Nanoemulgel, i.e., 10, 50, and 100 µg/mL. At 0.5, 4, and 10 h, the percentage of hemolysis was examined, along with the impact of the therapy on RBCs. The findings revealed that the rate of RBC hemolysis was significantly reduced when treated with QF-NE and QF-Nanoemulgel compared to 0.01 % SLS and QF-suspension due to the limited production of oxyhemoglobin levels. Additionally, after 10 h treatment with a higher concentration (100 µg/mL), the QF-Nanoemulgel formulations demonstrated significantly lower hemolysis (<0.5 %) compared to QF-Suspension and QF-NE (Fig. 6A and 6B). This is due to the surface effect of chitosan poloxamer-coated nanoparticles, which has a protective effect on erythrocytes to reduce the oxidative stress caused by QF agents. Consequently, all QF nanoformulations had substantially less potential to induce hemolysis than plain QF-Suspension and 0.01 % SLS. This preliminary investigation focuses on the hemolytic evidence as previously described (Fan et al., 2015), namely hemolytic anemia and thrombocytopenia, a severe adverse event of QF. Finally, the results demonstrated the biodegradability, biocompatibility, and acceptability of the proposed NE formulations for human application, potentially reducing the hemolytic impact of QF.

3.5.8. Stability evaluation

According to ICH guidelines, an accelerated stability experiment was carried out, and the globule size, % Transmittance, PDI, zeta potential, and % EE for optimized formulations were evaluated. There was no substantial change in the test findings and no indications of instability because all the quality control parameters were within acceptable limits (Table 4). As a result, optimized formulations of QF-NE and QF-Nanoemulgel exhibited remarkable stability.

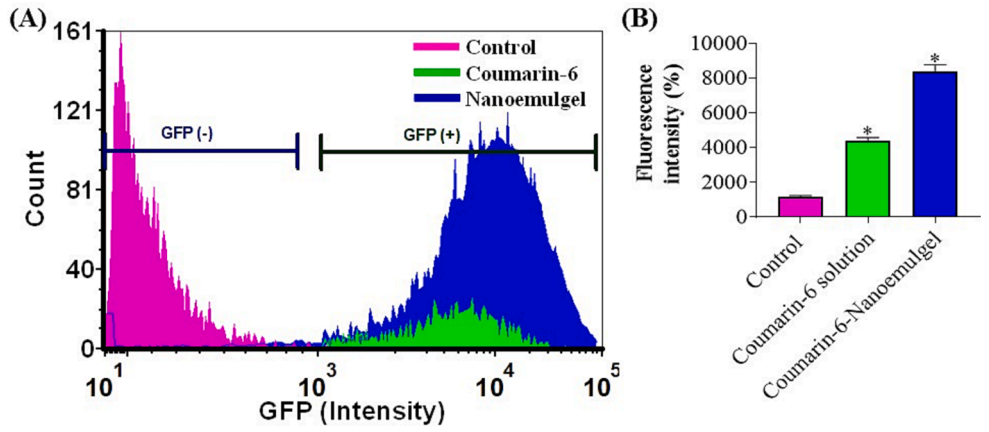

(C)

Formulation	Green fluorescence protein % of cells (+)	Fluorescence intensity geometric mean
Control RPMI-2650 cells	0.26 ± 0.04	1183.9 ± 49
Coumarin-6 solution	78.7 ± 2.6	4377.6 ± 201
Coumarin-6-Nanoemulgel	94.64 ± 3.2	8361.7 ± 412

Fig. 9. **(A)** Quantitative representation of fluorescence intensities by Cellometer Vision, **(B)** internalization of fluorescence and its intensity in RPMI0-2650 cells and **(C)** findings from Nexcelom Cellometer analysis based on fluorescence intensity for control RPMI-2650 cells, Coumarin-6 solution and Coumarine-6-Nanoemulgel. Data expressed as mean ± SD ($n = 3$) *$p < 0.05$.

3.6. Cell culture experiments

3.6.1. In-vitro cytotoxicity of developed Nanoemulgel formulation

This study was performed to depict the safety of the QF-Nanoemulgel on human nasal epithelial cell line RPMI-2650. The safety of QF seems to have improved through biodegradable cationic Nanoemulgel, and cellular toxicity did not follow being treated with the highest concentrations "25 μM" of the QF-Nanoemulgel. Subsequently, treatment was then carried out at different time points, i.e., 12 h and 24 h; the cytotoxicity of QF-Nanoemulgel is shown in Fig. 7. The long-term (24 h) treatment with 25 μM of Pure QF, Blank-Nanoemulgel, and QF-Nanoemulgel showed 81.4 ± 2.5, 74.9 ± 3.3, and 72.6 ± 2.7 % cell viability, respectively **(**Fig. 7**A)**. However, Fig. 7**B** represented higher viability, 88.3 ± 1.7, 84.1 ± 3.4, and 81.2 ± 2.5 %, at subsequent 12 h treatment with 25 μM of Pure QF, Blank-Nanoemulgel, and QF-Nanoemulgel, respectively. Outcomes supported that the developed QF-Nanoemulgel did not induce cytotoxicity after being treated with a higher dose (25 μM). Additionally, the cytotoxicity results for 4 h treatment with QF-Nanoemulgel are depicted in **Fig. S3**, which also demonstrated similar patterns. This study was performed to demonstrate the safety of QF-Nanoemulgel for permeation study **(Fig. S3)**. Hence, the developed Nanoemulgel was highly safe against RPMI-2650 nasal epithelial cell lines.

3.6.2. In-vitro cellular uptake of Nanoemulgel by fluorescence microscopy

Coumarin-6-Nanoemulgel was formulated to assess the uptake of Nanoemulgel in the intracellular environment. Generally, coumarin-6 release was observed slowly; therefore, this work intended to improve the release and uptake of coumarin-6 by nanoparticles. Cellular uptake analysis shows complete nanoparticle uptake by cells in an aqueous extracellular environment. Fig. 8A-D represented qualitative fluorescence images of RPMI-2650 cells combined with coumarin-6-Nanoemulgel for 1 **(**Fig. 8**A-B)** and 3 h **(**Fig. 8**C-D)**, respectively. The fluorescence images demonstrated that coumarin-6-Nanoemulgel revealed higher uptake than the control. It was also shown that coumarin-6-Nanoemulgel localized in the cells for an extended time with maximum fluorescence intensity, which was found after 1 and 3 h of treatment. The outcomes ensure the highest uptake of chitosan-poloxamer-coated cationic Nanoemulgel, emphasizing the controlled release capability of Nanoemulgel formulation in cellular environments.

3.6.3. In-vitro cellular uptake via Nexcelom Cellometer Vision

Further, to quantify the effect of Nanoemulgel on cellular uptake, cells were treated with Coumarin-6-Nanoemulgel and coumarin-6 solution for 3 h prior to fluorescence intensity evaluation. Quantitative illustration of *in-vitro* cellular uptake for control, coumarin-6 solution and coumarin-6-Nanoemulgel by Cellometer vision are depicted in **Fig. S4**. Additionally, Fig. 9A & 9B represented the mean fluorescence intensity for different coumarin-6-loaded formulations, where pink color represents control cell lines (without being treated with coumarin-6), green color depicts cell lines treated with coumarin-6 solution, and blue color indicates cell lines treated with coumarin-6-Nanoemulgel. The findings suggested that mean fluorescence intensity stabilized after treatment with coumarin-6-Nanoemulgel formulation, and > 2-fold uptake was confirmed than the coumarin-6 solution. The mean fluorescence intensity and green fluorescence intensity are represented in Fig. 9C. Interaction between the cationic charge of Nanoemulgel and the anionic surface of the cell membrane may demonstrate why cationic nanoparticles are more easily absorbed. Therefore, chitosan-poloxamer as a cationic polymer makes cellular uptake more feasible. Consequently, Nanoemulgel globules coated with chitosan and poloxamer having a more significant positive charge (+21.5 mV) always showed an excellent uptake profile (Vaidya et al., 2020).

3.6.4. QF permeation across RPMI-2650 cells

Human nasal epithelial cells RPMI-2650 were utilized to assess the QF permeation potential of developed QF-Nanoemulgel. Before the investigation, RPMI-2650 was incubated in EMEM for 16 days to promote the growth of cellular monolayer tissue. TEER values were measured for 1 and 16 incubation days and were revealed as 42.5 Ωcm^2 and 85.4 Ωcm^2, respectively (Fig. 10**A)**. After an incubation period of 3 h, QF permeability study showed that 0.55 ± 0.02 and 1.1 ± 0.04 μg of QF were permeated by 12.5 and 25 μM QF-Nanoemulgel across Transwell™, respectively. At the same time, 0.46 ± 0.04 μg/cm^2 and 0.92 ± 0.05 μg of QF released through pure QF solution after 3 h **(**Fig. 10**B & 10C)**. Consequently, in-situ gelling approach reveals a slightly better QF

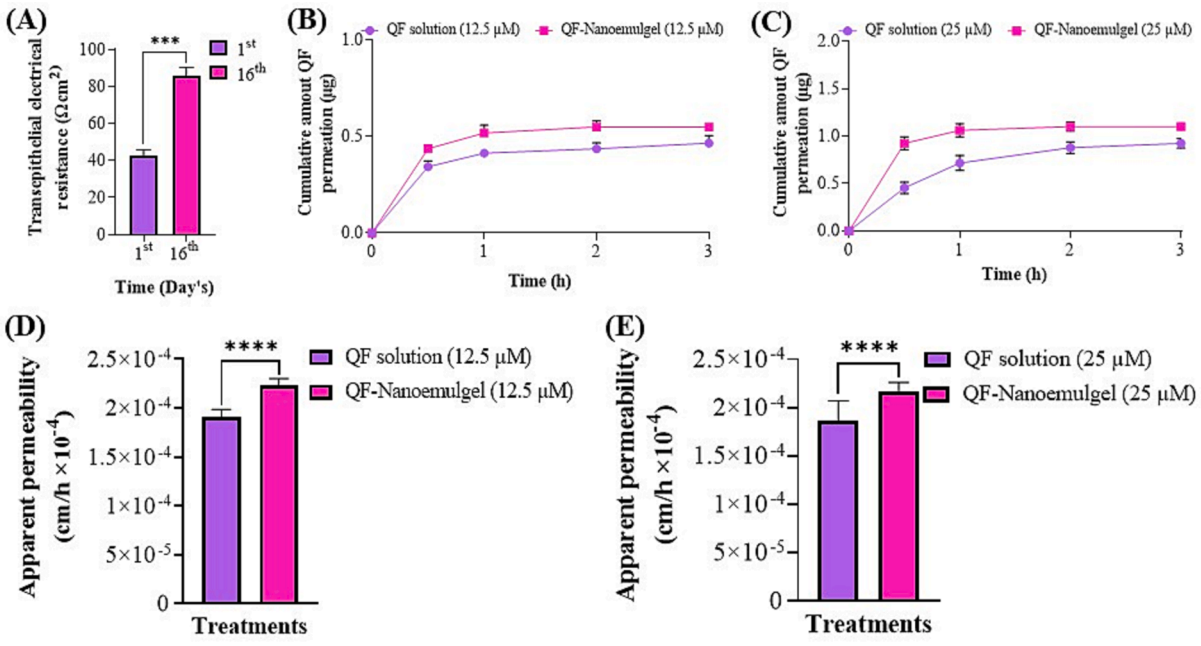

(F)

Formulations	Flux J_{ss} (µg/cm²/h)	Permeability coefficient P_{app} (cm/h × 10^{-4})	Cumulative QF permeated at 3 h (µg)
QF Solution (12.5 µM)	1.04 ± 0.2	1.90 ± 0.1	0.466 ± 0.03
QF Solution (25 µM)	2.05 ± 0.3	1.86 ± 0.3	0.923 ± 0.04
QF-Nanoemulgel (12.5 µM)	1.22 ± 0.4	2.22 ± 0.2	0.550 ± 0.03
QF-Nanoemulgel (25 µM)	2.38 ± 0.5	2.16 ± 0.4	1.100 ± 0.04

Fig. 10. **(A)** Transepithelial electrical resistance (TEER) value for RPMI-2650 monolayer on Transwell™ after 1st and 16th day of incubation. Cumulative amount of QF permeated across the RPMI-2650 epithelial cell line incubated on Transwell™ inserts after 3 h treatment from **(B)** 12.5 and **(C)** 25 µM of QF solution and QF-Nanoemulgel. Apparent permeability of **(D)** 12.5 and **(E)** 25 µM QF solution and QF-Nanoemulgel and **(F)** Permeation results of QF, permeated across the nasal epithelial cells RPMI-2650 (concentration of QF in donor chamber, $Cd = 0.5$ and 1.1 µg/mL and volume of NPs in donor compartment, $Vd = 100$ µL). Data expressed as mean ± SD ($n = 3$). **p < 0.01, ***p < 0.005 and ****p < 0.001.

permeation than the QF solution. These results are due to the mucoadhesive agent helping to enhance nasal residence time; hence the rapid drug permeation occurred through QF-Nanoemulgel formulation (Kumbhar et al., 2020; Pathak et al., 2014; Vaz et al., 2022). Even cationic nano globules easily interact with the anionic cell surface and easily permeate across the cell membrane. Further, the QF solution is free from mucoadhesive/gelling agents which can lead to partial drug permeation across the nasal mucosa. The solution retards QF permeation across the RPMI-2650-coated Transwell™. Comparative examination of apparent permeability coefficient (P_{app}) and steady-state flux (J_{ss}) were performed for QF-Nanoemulgel formulations for 3 h. The QF-Nanoemulgel exhibited higher P_{app} (2.16 ± 0.4 cm/h × 10^{-4}) and J_{ss} (2.38 ± 0.5 µg/cm²/h), compared to P_{app} (1.86 ± 0.3 cm/h × 10^{-4}) and J_{ss} (2.05 ± 0.3 µg/cm²/h) of QF solutions (Fig. 10**D-F**). Wherein, charge transformation is applicable for opening tight junctions of the mucous membrane, enhancing the permeation of therapeutics toward the target. Consequently, chitosan and poloxamer-coated cationic Nanoemulgel have the potential to permeate across the barriers. Although, the outcomes of the permeation analysis demonstrated that biodegradable QF-Nanoemulgel has the strength to avoid mucociliary clearance of nasal mucosa (reflux mechanism of the nose) and help to permeate QF across the membrane safely. It could overcome the limitation of BBB and improve QF permeation towards the CNS.

4. Conclusions

Current research aims to enhance QF intranasal permeability and physicochemical stability to enhance absorption and therapeutic efficacy in mental illnesses. A noninvasive approach for IN drug administration for QF, an antipsychotic agent, was designed by formulation of ISG utilizing ionic and thermo-responsive components. It was demonstrated that this cutting-edge drug delivery technique could circumvent BBB hindrance and deliver QF directly to the CNS. Biodegradable Nanoemulgel has the potential to reduce dose, dosing frequency, and related toxicities, facilitating effective delivery of therapeutic to the brain by IN route. Additionally, the QF-Nanoemulgel in-vitro release showed constant drug release in SNES over 24 h, which could assess the prolonged delivery of QF to the brain. The ex-vivo hemolysis investigation demonstrated that the developed Nanoemulgel showed no hemolytic symptoms compared to pure QF and negative control. However, in-vitro cytotoxicity tests against RPMI-2650 human nasal epithelial cells revealed the safety of QF-Nanoemulgel over pure QF. While the reduced mucociliary clearance might enhance QF transport through the nasal epithelium, increasing QF permeability across RPMI-2650 cells in the presence of biodegradable Nanoemulgel. As a result, CSN delivery of antipsychotics by Nanoemulgel has been successfully proposed, which may lead to a bright future for the safe, effective, and economical treatment of schizophrenia.

Funding

This work was supported with research funds of VG by the College of

Pharmacy and Health Sciences, St. John's University, Queens, DGG was supported with pharmaceutical industry research funds to VG of St. John's University.

Declaration of Competing Interest

The authors declare that they have no known competing financial interests or personal relationships that could have appeared to influence the work reported in this paper.

Data availability

Data will be made available on request.

Appendix A. Supplementary data

Supplementary data to this article can be found online at https://doi.org/10.1016/j.ijpharm.2023.123566.

References

Ahmad, N., 2017. Rasagiline-encapsulated chitosan-coated PLGA nanoparticles targeted to the brain in the treatment of parkinson's disease. J. Liq. Chromatogr. Relat. Technol. 40, 677–690. https://doi.org/10.1080/10826076.2017.1343735.

Ahmad, S., Khan, I., Pandit, J., Emad, N.A., Bano, S., Dar, K.I., Rizvi, M.M.A., Ansari, M. D., Aqil, M., Sultana, Y., 2022. Brain targeted delivery of carmustine using chitosan coated nanoparticles via nasal route for glioblastoma treatment. Int. J. Biol. Macromol. 221, 435–445. https://doi.org/10.1016/j.ijbiomac.2022.08.210.

Alaayedi, M.H., Maraie, N.K., 2023. Lomustine's nanoemulsion as nose-to-brain drug delivery system for CNS tumor treatment. Saudi Pharmaceutical Journal 31, 101692. https://doi.org/10.1016/j.jsps.2023.06.025.

Alqahtani, S., Simon, L., Astete, C.E., Alayoubi, A., Sylvester, P.W., Nazzal, S., Shen, Y., Xu, Z., Kaddoumi, A., Sabliov, C.M., 2015. Cellular uptake, antioxidant and antiproliferative activity of entrapped α-tocopherol and γ-tocotrienol in poly (lactic-co-glycolic) acid (PLGA) and chitosan covered PLGA nanoparticles (PLGA-Chi). Journal of Colloid and Interface Science 445, 243–251. https://doi.org/10.1016/j.jcis.2014.12.083.

Arslan, F.C., Aykut, D.S., Ince, C., Tiryaki, A., 2016. Neutropenia and Thrombocytopenia Induced By Quetiapine Monotherapy: A Case Report and Review of Literature. Klinik Psikofarmakoloji Bülteni-Bulletin of Clinical Psychopharmacology 26, 319–323. https://doi.org/10.5455/bcp.20151219072235.

Banks, W.A., 2012. Drug delivery to the brain in Alzheimer's disease: Consideration of the blood–brain barrier. Adv. Drug Deliv. Rev. 64, 629–639. https://doi.org/10.1016/j.addr.2011.12.005.

Bhavna, M.d., S., Ali, M., Ali, R., Bhatnagar, A., Baboota, S., Ali, J.,, 2014. Donepezil nanosuspension intended for nose to brain targeting: In vitro and in vivo safety evaluation. International Journal of Biological Macromolecules 67, 418–425. https://doi.org/10.1016/j.ijbiomac.2014.03.022.

Bruinsmann, F.A., Alves, D.C.S., A., De Fraga Dias, A., Lopes Silva, L.F., Visioli, F., Raffin Pohlmann, A., Figueiró, F., Sonvico, F., Stanisçuaski Guterres, S.,, 2022. Nose-to-brain delivery of simvastatin mediated by chitosan-coated lipid-core nanocapsules allows for the treatment of glioblastoma in vivo. International Journal of Pharmaceutics 616, 121563. https://doi.org/10.1016/j.ijpharm.2022.121563.

Chatzitaki, A.-T., Jesus, S., Karavasili, C., Andreadis, D., Fatouros, D.G., Borges, O., 2020. Chitosan-coated PLGA nanoparticles for the nasal delivery of ropinirole hydrochloride: In vitro and ex vivo evaluation of efficacy and safety. Int. J. Pharm. 589, 119776 https://doi.org/10.1016/j.ijpharm.2020.119776.

Cho, H.-J., Balakrishnan, P., Park, E.-K., Song, K.-W., Hong, S.-S., Jang, T.-Y., Kim, K.-S., Chung, S.-J., Shim, C.-K., Kim, D.-D., 2011. Poloxamer/Cyclodextrin/Chitosan-Based Thermoreversible Gel for Intranasal Delivery of Fexofenadine Hydrochloride. J. Pharm. Sci. 100, 681–691. https://doi.org/10.1002/jps.22314.

Choudhury, H., Zakaria, N.F.B., Tilang, P.A.B., Tzeyung, A.S., Pandey, M., Chatterjee, B., Alhakamy, N.A., Bhattamishra, S.K., Kesharwani, P., Gorain, B., Md, S., 2019. Formulation development and evaluation of rotigotine mucoadhesive nanoemulsion for intranasal delivery. J. Drug Delivery Sci. Technol. 54, 101301 https://doi.org/10.1016/j.jddst.2019.101301.

Crépeau-Gendron, G., L'Heureux, S., 2015. Quetiapine XR-induced neutropenia: is a clozapine trial still possible for treatment-resistant schizophrenia? A case report: Clozapine after quetiapine XR-induced neutropenia. Early Interv. Psychiatry 9, 151–155. https://doi.org/10.1111/eip.12134.

Cunha, S., Swedrowska, M., Bellahnid, Y., Xu, Z., Sousa Lobo, J.M., Forbes, B., Silva, A. C., 2022. Thermosensitive in situ hydrogels of rivastigmine-loaded lipid-based nanosystems for nose-to-brain delivery: characterisation, biocompatibility, and drug deposition studies. Int. J. Pharm. 620, 121720 https://doi.org/10.1016/j.ijpharm.2022.121720.

Fan, K.-Y., Chen, W.-Y., Huang, M.-C., 2015. Quetiapine-associated leucopenia and thrombocytopenia: a case report. BMC Psychiatry 15, 110. https://doi.org/10.1186/s12888-015-0495-9.

Fornaguera, C., Dols-Perez, A., Calderó, G., García-Celma, M.J., Camarasa, J., Solans, C., 2015. PLGA nanoparticles prepared by nano-emulsion templating using low-energy methods as efficient nanocarriers for drug delivery across the blood–brain barrier. J. Control. Release 211, 134–143. https://doi.org/10.1016/j.jconrel.2015.06.002.

Gadhave, D., Choudhury, H., Kokare, C., 2019a. Neutropenia and leukopenia protective intranasal olanzapine-loaded lipid-based nanocarriers engineered for brain delivery. Appl Nanosci 9, 151–168. https://doi.org/10.1007/s13204-018-0909-3.

Gadhave, D., Gorain, B., Tagalpallewar, A., Kokare, C., 2019b. Intranasal teriflunomide microemulsion: An improved chemotherapeutic approach in glioblastoma. J. Drug Delivery Sci. Technol. 51, 276–289. https://doi.org/10.1016/j.jddst.2019.02.013.

Gadhave, D.G., Kokare, C.R., 2019. Nanostructured lipid carriers engineered for intranasal delivery of teriflunomide in multiple sclerosis: optimization and *in vivo* studies. Drug Dev. Ind. Pharm. 45, 839–851. https://doi.org/10.1080/03639045.2019.1576724.

Gadhave, D., Rasal, N., Sonawane, R., Sekar, M., Kokare, C., 2021a. Nose-to-brain delivery of teriflunomide-loaded lipid-based carbopol-gellan gum nanogel for glioma: Pharmacological and in vitro cytotoxicity studies. Int. J. Biol. Macromol. 167, 906–920. https://doi.org/10.1016/j.ijbiomac.2020.11.047.

Gadhave, D., Tupe, S., Tagalpallewar, A., Gorain, B., Choudhury, H., Kokare, C., 2021b. Nose-to-brain delivery of amisulpride-loaded lipid-based poloxamer-gellan gum nanoemulgel: In vitro and in vivo pharmacological studies. Int. J. Pharm. 607, 121050 https://doi.org/10.1016/j.ijpharm.2021.121050.

Gadhave, D., Khot, S., Tupe, S., Shinde, M., Tagalpallewar, A., Gorain, B., Kokare, C., 2022. Nose-to-brain delivery of octreotide acetate in situ gel for pituitary adenoma: Pharmacological and in vitro cytotoxicity studies. Int. J. Pharm. 629, 122372 https://doi.org/10.1016/j.ijpharm.2022.122372.

Gadhave, D., Gupta, A., Khot, S., Tagalpallewar, A., Kokare, C., 2023. Nose-to-brain delivery of paliperidone palmitate poloxamer-guar gum nanogel: Formulation, optimization and pharmacological studies in rats. Ann. Pharm. Fr. 81, 315–333. https://doi.org/10.1016/j.pharma.2022.08.010.

Godara, S., Lather, V., Kirthanashri, S.V., Awasthi, R., Pandita, D., 2020. Lipid-PLGA hybrid nanoparticles of paclitaxel: Preparation, characterization, in vitro and in vivo evaluation. Mater. Sci. Eng. C 109, 110576. https://doi.org/10.1016/j.msec.2019.110576.

Gonçalves, V.S.S., Matias, A.A., Poejo, J., Serra, A.T., Duarte, C.M.M., 2016. Application of RPMI 2650 as a cell model to evaluate solid formulations for intranasal delivery of drugs. International Journal of Pharmaceutics 515, 1–10. https://doi.org/10.1016/j.ijpharm.2016.09.086.

Jeswani, G., Chablani, L., Gupta, U., Sahoo, R.K., Nakhate, K.T., Ajazuddin,, 2021. Development and optimization of paclitaxel loaded Eudragit/PLGA nanoparticles by simplex lattice mixture design: Exploration of improved hemocompatibility and in vivo kinetics. Biomed. Pharmacother. 144, 112286 https://doi.org/10.1016/j.biopha.2021.112286.

Kokare, C., Koli, D., Gadhave, D., Mote, C., Khandekar, G., 2020. Efavirenz-loaded intranasal microemulsion for crossing blood-CNS interfaces in neuronal-AIDS: pharmacokinetic and *in vivo* safety evaluation. Pharm. Dev. Technol. 25, 28–39. https://doi.org/10.1080/10837450.2019.1659818.

Kumbhar, S.A., Kokare, C.R., Shrivastava, B., Gorain, B., Choudhury, H., 2020. Preparation, characterization, and optimization of asenapine maleate mucoadhesive nanoemulsion using Box-Behnken design: In vitro and in vivo studies for brain targeting. Int. J. Pharm. 586, 119499 https://doi.org/10.1016/j.ijpharm.2020.119499.

Kumbhar, S.A., Kokare, C.R., Shrivastava, B., Gorain, B., Choudhury, H., 2021. Antipsychotic Potential and Safety Profile of TPGS-Based Mucoadhesive Aripiprazole Nanoemulsion: Development and Optimization for Nose-To-Brain Delivery. J. Pharm. Sci. 110, 1761–1778. https://doi.org/10.1016/j.xphs.2021.01.021.

Ladel, S., Schlossbauer, P., Flamm, J., Luksch, H., Mizaikoff, B., Schindowski, K., 2019. Improved In Vitro Model for Intranasal Mucosal Drug Delivery: Primary Olfactory and Respiratory Epithelial Cells Compared with the Permanent Nasal Cell Line RPMI 2650. Pharmaceutics 11, 367. https://doi.org/10.3390/pharmaceutics11080367.

Li, X., Cameron, M.D., 2012. Potential Role of a Quetiapine Metabolite in Quetiapine-Induced Neutropenia and Agranulocytosis. Chem. Res. Toxicol. 25, 1004–1011. https://doi.org/10.1021/tx2005635.

Mura, P., Mennini, N., Nativi, C., Richichi, B., 2018. In situ mucoadhesive-thermosensitive liposomal gel as a novel vehicle for nasal extended delivery of opiorphin. Eur. J. Pharm. Biopharm. 122, 54–61. https://doi.org/10.1016/j.ejpb.2017.10.008.

Parvathaneni, V., Kulkarni, N.S., Chauhan, G., Shukla, S.K., Elbatanony, R., Patel, B., Kunda, N.K., Muth, A., Gupta, V., 2020. Development of pharmaceutically scalable inhaled anti-cancer nanotherapy – Repurposing amodiaquine for non-small cell lung cancer (NSCLC). Mater. Sci. Eng. C 115, 111139. https://doi.org/10.1016/j.msec.2020.111139.

Parvathaneni, V., Shukla, S.K., Kulkarni, N.S., Gupta, V., 2021. Development and characterization of inhalable transferrin functionalized amodiaquine nanoparticles – Efficacy in Non-Small Cell Lung Cancer (NSCLC) treatment. Int. J. Pharm. 608, 121038 https://doi.org/10.1016/j.ijpharm.2021.121038.

Pathak, R., Prasad Dash, R., Misra, M., Nivsarkar, M., 2014. Role of mucoadhesive polymers in enhancing delivery of nimodipine microemulsion to brain via intranasal route. Acta Pharm. Sin. B 4, 151–160. https://doi.org/10.1016/j.apsb.2014.02.002.

Qu, Y., Li, A., Ma, L., Iqbal, S., Sun, X., Ma, W., Li, C., Zheng, D., Xu, Z., Zhao, Z., Ma, D., 2021. Nose-to-brain delivery of disulfiram nanoemulsion in situ gel formulation for glioblastoma targeting therapy. Int. J. Pharm. 597, 120250 https://doi.org/10.1016/j.ijpharm.2021.120250.

Radivojša, M., Grabnar, I., Ahlin Grabnar, P., 2013. Thermoreversible in situ gelling poloxamer-based systems with chitosan nanocomplexes for prolonged subcutaneous delivery of heparin: Design and in vitro evaluation. European Journal of Pharmaceutical Sciences, Emerging Nanopharmaceuticals for Non-Parenteral Application Routes 50, 93–101. https://doi.org/10.1016/j.ejps.2013.03.002.

Raman, S., Khan, A.A., Mahmood, S., 2022. Nose to brain delivery of selegiline loaded PLGA/lipid nanoparticles: Synthesis, characterisation and brain pharmacokinetics evaluation. Journal of Drug Delivery Science and Technology 77, 103923. https://doi.org/10.1016/j.jddst.2022.103923.

Ravi Shankar, B., 2007. Quetiapine-Induced Leucopenia and Thrombocytopenia. Psychosomatics 48, 530–531. https://doi.org/10.1176/appi.psy.48.6.530.

Seju, U., Kumar, A., Sawant, K.K., 2011. Development and evaluation of olanzapine-loaded PLGA nanoparticles for nose-to-brain delivery: In vitro and in vivo studies. Acta Biomater. 7, 4169–4176. https://doi.org/10.1016/j.actbio.2011.07.025.

Shah, B., Khunt, D., Misra, M., Padh, H., 2016. Non-invasive intranasal delivery of quetiapine fumarate loaded microemulsion for brain targeting: Formulation, physicochemical and pharmacokinetic consideration. Eur. J. Pharm. Sci. 91, 196–207. https://doi.org/10.1016/j.ejps.2016.05.008.

Shukla, K., S., Nguyen, V., Goyal, M., Gupta, V.,, 2022. Cationically modified inhalable nintedanib niosomes: enhancing therapeutic activity against non-small-cell lung cancer. Nanomedicine 17, 935–958. https://doi.org/10.2217/nnm-2022-0045.

Sibinovska, N., Žakelj, S., Kristan, K., 2019. Suitability of RPMI 2650 cell models for nasal drug permeability prediction. Eur. J. Pharm. Biopharm. 145, 85–95. https://doi.org/10.1016/j.ejpb.2019.10.008.

Tarik Alhamdany, A., Saeed, A.M.H., Alaayedi, M., 2021. Nanoemulsion and Solid Nanoemulsion for Improving Oral Delivery of a Breast Cancer Drug: Formulation, Evaluation, and a Comparison Study. Saudi Pharmaceutical Journal 29, 1278–1288. https://doi.org/10.1016/j.jsps.2021.09.016.

Tong, G.-F., Qin, N., Sun, L.-W., 2017. Development and evaluation of Desvenlafaxine loaded PLGA-chitosan nanoparticles for brain delivery. Saudi Pharmaceutical Journal 25, 844–851. https://doi.org/10.1016/j.jsps.2016.12.003.

Vaidya, B., Parvathaneni, V., Kulkarni, N.S., Shukla, S.K., Damon, J.K., Sarode, A., Kanabar, D., Garcia, J.V., Mitragotri, S., Muth, A., Gupta, V., 2019. Cyclodextrin modified erlotinib loaded PLGA nanoparticles for improved therapeutic efficacy against non-small cell lung cancer. Int. J. Biol. Macromol. 122, 338–347. https://doi.org/10.1016/j.ijbiomac.2018.10.181.

Vaidya, B., Kulkarni, N.S., Shukla, S.K., Parvathaneni, V., Chauhan, G., Damon, J.K., Sarode, A., Garcia, J.V., Kunda, N., Mitragotri, S., Gupta, V., 2020. Development of inhalable quinacrine loaded bovine serum albumin modified cationic nanoparticles: Repurposing quinacrine for lung cancer therapeutics. Int. J. Pharm. 577, 118995 https://doi.org/10.1016/j.ijpharm.2019.118995.

Van De Ven, H., Paulussen, C., Feijens, P.B., Matheeussen, A., Rombaut, P., Kayaert, P., Van Den Mooter, G., Weyenberg, W., Cos, P., Maes, L., Ludwig, A., 2012. PLGA nanoparticles and nanosuspensions with amphotericin B: Potent in vitro and in vivo alternatives to Fungizone and Am Bisome. J. Control. Release 161, 795–803. https://doi.org/10.1016/j.jconrel.2012.05.037.

Vaz, G., Clementino, A., Mitsou, E., Ferrari, E., Buttini, F., Sissa, C., Xenakis, A., Sonvico, F., Dora, C.L., 2022. In Vitro Evaluation of Curcumin- and Quercetin-Loaded Nanoemulsions for Intranasal Administration: Effect of Surface Charge and Viscosity. Pharmaceutics 14, 194. https://doi.org/10.3390/pharmaceutics14010194.

Wang, X., Parvathaneni, V., Shukla, S.K., Kulkarni, N.S., Muth, A., Kunda, N.K., Gupta, V., 2020. Inhalable resveratrol-cyclodextrin complex loaded biodegradable nanoparticles for enhanced efficacy against non-small cell lung cancer. Int. J. Biol. Macromol. 164, 638–650. https://doi.org/10.1016/j.ijbiomac.2020.07.124.

Wilson, B., Mohamed Alobaid, B.N., Geetha, K.M., Jenita, J.L., 2021. Chitosan nanoparticles to enhance nasal absorption and brain targeting of sitagliptin to treat Alzheimer's disease. J. Drug Delivery Sci. Technol. 61, 102176 https://doi.org/10.1016/j.jddst.2020.102176.

Yu, Y., Feng, R., Yu, S., Li, J., Wang, Y., Song, Y., Yang, X., Pan, W., Li, S., 2018. Nanostructured lipid carrier-based pH and temperature dual-responsive hydrogel composed of carboxymethyl chitosan and poloxamer for drug delivery. Int. J. Biol. Macromol. 114, 462–469. https://doi.org/10.1016/j.ijbiomac.2018.03.117.

Zhou, C., Xue, S., Xue, F., Liu, L., Liu, J., Ma, Q., Qin, J., Tan, Q., Wang, H., Peng, Z., 2020. The impact of quetiapine on the brain lipidome in a cuprizone-induced mouse model of schizophrenia. Biomedicine & Pharmacotherapy 131, 110707. https://doi.org/10.1016/j.biopha.2020.110707.